UK Health Security Agency

Variation in Absorbed Dose Rate to the Skin from Exposure by Small Radioactive Objects

MCNP Calculations using ICRP Skin Model

RCEHD-RAD-2024-01

VERSION 1.0

Contents

Extended summary

Small discrete objects, ranging in size from less from than 1 mm to several cm, contaminated with radioactivity have been found in several locations in the UK, including on beaches near Sellafield, Dounreay and Dalgety Bay (Environment Agency et al, 2022). One of the main health hazards posed by these objects is the potential development of severe tissue reactions in the skin. The risk to people's health was assessed in Oatway et al (2020a), but there is still uncertainty about how the nature of the object and the exposed person affects the dose received. This report investigates how various factors affect the dose.

To calculate the dose rate to skin from these objects, several assumptions need to be made about the nature of the radiation exposure and the location of radiosensitive cells within the skin. The location of radiosensitive cells within the skin varies for different parts of the body and with the age of an individual. Therefore, the International Commission on Radiological Protection (ICRP) have recommended for radiation protection purposes that the dose rate to the skin is estimated at a depth of 70 μm or between 50 μm and 100 μm and over an area of 1 cm^2. This approach has also been applied to exposure from radioactive objects.

To investigate the impact of this ICRP approach when exposure is from radioactivity on small objects, the study described in this report used the Monte Carlo particle transport software MCNP (Goorley et al, 2012) to simulate an exposure to the skin. As part of the study the location (as a point source or distributed through an object) and type of the radiation source was varied, and the absorbed dose rate calculated at a series of skin depths.

This work showed that photons deposit energy at all depths of skin and therefore assumptions made about the depth of the radiosensitive cells within the skin do not have a significant effect on the dose: for such shallow depths the inverse square attenuation of the field is not a strong effect. The study found that there was more variation in the dose rate caused by electrons of low initial energies (<0.3 MeV) at different depths of skin, reflecting the range in skin of the primary electrons. Graphs of absorbed dose rate versus skin depth for a series of source energies can be found in appendix A.

It was found that most alpha particles rarely penetrate the skin by more than a few tens of micrometres, shallower than the depths normally considered in radiation protection. Consequently, they are often not considered in skin dose assessments. However, radiosensitive cells are closer to the surface of the skin in some parts of the body and for some individuals, and this work showed that higher energy alpha particles, including those emitted by ^{241}Am, and ^{226}Ra, can penetrate the skin to depths equivalent to the lower end of the range occupied by of radiosensitive cells as defined by ICRP. The ICRP has also reported doses from alpha particles at the shallower depth of 16 μm and found elevated incidence, compared to the general public, of skin cancers in uranium miners with greater than ten years of exposure (ICRP, 1991b). While this work demonstrates that exposures to radionuclides emitting high energy alpha particles have the potential to cause severe tissue reactions in skin, it is recognised that any such damage is likely to be limited to acute ulceration and will not threaten the overall health of the individual.

The distribution of the radionuclides in the object and the density of the object were found to be important factors in the dose rate to the skin. Only radionuclides in close contact with the skin are likely to result in alpha penetration of the skin.

This work was undertaken under the Radiation Assessments Department's Quality Management System, which has been approved by Lloyd's Register to the Quality Management Standard ISO 9001:2015, Approval No: ISO 9001 - 00002655.

Report Version 1.0

1 Introduction

Small radioactive objects have been found at locations across the UK primarily associated with historical discharges of radioactivity from nuclear installations, for example, around the Sellafield and Dounreay nuclear licensed sites (Oatway et al, 2020a; Particles Retrieval Advisory Group (Dounreay), 2012) or with the manufacture, maintenance, and disposal of radium luminised instruments which occurred widely between the 1920s and 1960s, for example at Dalgety Bay (COMARE, 2014). The objects present at these locations range in size from less than a millimetre to several centimetres and are composed of a variety of materials. Different radionuclides may be present on them, with ^{90}Sr, ^{137}Cs, ^{226}Ra, ^{241}Am and isotopes of plutonium, together with their radioactive progeny, being frequently detected.

The main risk to health posed by these small radioactive objects is from irradiation of the gastrointestinal tract following ingestion, which may also include prolonged exposure of other organs and tissues following uptake across the gut wall, and exposure to the skin when an object is in direct, prolonged, and stationary contact with it (COMARE, 2014; Oatway et al, 2020a; Particles Retrieval Advisory Group (Dounreay), 2012). This report is focussed on developing our understanding of how the dose to the skin is derived from being irradiated by a specific object. The probability of encountering such an object was estimated as very low in Oatway et al (2020b) though objects with activities greater than 100 kBq have been detected on beaches near Sellafield.

Exposure of the skin to radiation presents potential health risks from the development erythema, desquamation, ulceration, and longer-term skin cancer. Acute damage due to direct cell-killing is categorised as a tissue reaction by the International Commission on Radiological Protection (ICRP) (ICRP, 2007; ICRP, 2012). These tissue reactions occur only above dose thresholds, with erythema induced above 2 Gy and moist desquamation above 18 Gy (Jaschke et al, 2017).

1.1 Structure of the skin

The skin can be divided into the outer epidermis layer and a deeper layer known as the dermis. The epidermis itself can be split into several layers with the dead cells of the stratum corneum forming the outer surface of the skin, and the basal layer at the bottom containing stem cells that continually produce new cells to replace the dead ones being lost from the outer surface. The basal layer undulates considerably with ridges or ‘rete pegs’ that project down into the dermis; the basal layer also extends around the roots of hair follicles (ICRP, 1992). It has been suggested (ICRP, 2015) that the origin of basal cell carcinoma, the main type of skin cancer induced by ionizing radiation, may predominantly originate in the intra-follicular basal cells and the base of the rete pegs. The typical depth of the basal layer over most areas of the body is between 20 μm and 100 μm although it can be more than 500 μm on the soles of the feet and the palms of the hands (Hopewell, 1990). The thickness of the epidermis also varies as a function of age: ICRP Publication 89 (ICRP, 2002) gives a reference thickness of 45 μm for a 1-year-old and 70 μm for an adult.

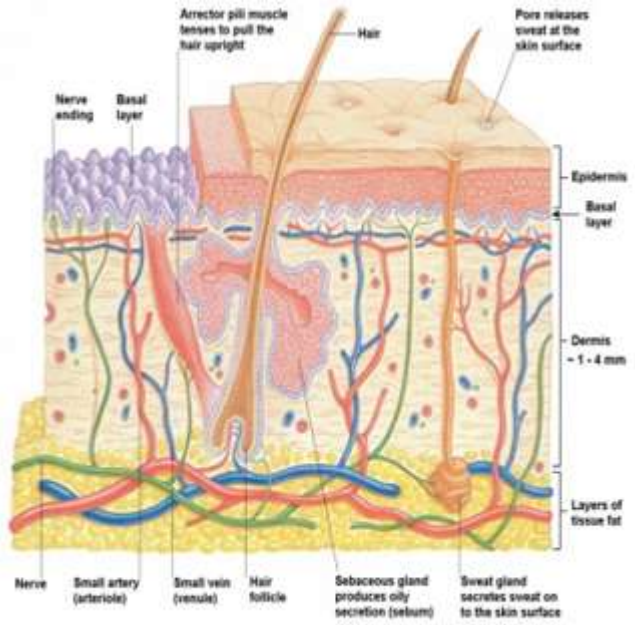

Figure 1: The layers of the skin from Harrison et al (2023)

In addition to the depth of sensitive cells within the skin, the size of the area of skin that is exposed to radiation is also important with respect to the potential occurrence of both tissue reactions and stochastic effects. For example, early experiments on pig skin allowed an estimate of the ED_{50} (the dose to produce an effect in 50% of individuals) for acute ulceration to be about 370 and 180 Gy for exposure from 1 and 2 mm particles respectively (NCRP, 1999), recognising that human skin appears to have a similar response to radiation as that observed in pigs (Dean et al, 1970; Kaurin et al, 1997; Kaurin et al, 2001). In addition, when estimating the risk of cancer developing in skin, the energy absorbed by the skin needs to be averaged over the mass of skin present on the body. Consequently, assuming a constant dose rate per unit area of skin, the risk that cancer may develop increases as the area of skin being irradiated increases.

The tissue reactions of the radiation exposure occur in several different stages, with an early erythema subsiding after 1 or 2 days, while dry desquamation, moist desquamation and/or hair loss developing several weeks later, the timing and severity of the effects depending on the severity of the exposure. Late skin damage effects include skin atrophy, telangiectasia and necrosis (ICRP, 1991b).

Alternative systems for the protection of skin from the effects of exposure to radiation have been suggested to take account of both the varying depth of basal cells and the area of skin exposed. This has included suggestions that doses should be calculated at a depth of 100 – 150 μm in evaluating an exposure to a small radioactive object and depths of 300 – 500 μm for dermal tissue reactions more generally (ICRP, 1991b). However, for radiation protection purposes, where the dose calculation has to account for variation of effects over different individuals and radiation types, ICRP have recommended to calculate and measure doses at a nominal depth of the epidermal basal layer of 70 μm, representing cells present between depths of 50 and 100 μm, for assessment of both tissue reactions and stochastic effects

(ICRP, 2007). To account for the range in area of skin that could be exposed, ICRP recommended that the risks to the skin should be estimated assuming the dose is that received over the most exposed 1 cm^2. While there is practical merit in adopting this approach, it has little biological significance in relation to exposure from small particles where no more than a few mm^2 of skin may be irradiated.

As alpha radiation is commonly assumed not to be able to penetrate skin to depths of 70 μm, and photons are assumed to deposit little energy in skin, for radiation protection purposes the absorbed dose rate to the skin is normally only assessed for exposure to beta emissions and discrete electrons. However, consideration of alpha radiation and, to a lesser extent, gamma radiation, may be important when those radiations are emitted from radionuclides present on small objects at high energy and in proximity to the skin surface.

This report describes a series of Monte Carlo simulations used to investigate the potential impact of irradiating skin by radionuclides present on small objects. The calculations described in this report include estimation of the absorbed dose rate at various depths of skin from radiation, first from point sources, then in objects of differing sizes located in direct contact with the skin. It also reviews the difference between dose rates calculated over an area of 1 cm^2 and 1.1 mm^2 to determine the relevance of averaging area on potential health consequence. The emitted radiation used in the modelling included mono-energetic alpha, beta and gamma rays and actual radiation spectra emitted by either ^{241}Am, ^{137}Cs, ^{90}Sr, ^{214}Po or ^{226}Ra, since these are the radionuclides most commonly encountered on small radioactive objects in the UK (Oatway et al, 2020a; Particles Retrieval Advisory Group (Dounreay), 2012).

2. Methodology

ICRP Publication 116 (ICRP, 2010) provides a model for assessing the local skin-equivalent dose. The model consists of a 10 cm ×10 cm × 10 cm cube of skin in which the density and elemental composition of the skin were taken from ICRP Publication 110 (ICRP, 2009). In additional to the ICRP model a cube of air was added above the skin to surround small objects on the skin surface and model the scatter of radiation back towards the skin surface.

The transport of particles through the skin was modelled using the Monte Carlo N-Particle (MCNP) version 6 software. The MCNP code, developed by Los Alamos National Laboratory (Goorley et al, 2012), simulates the transport of particles through materials, including the production and transport of secondary particles. The energy deposited by the radiations in the target cells was recorded in MCNP cells which are known as tallies.

The cubes of air and skin form the universe of the simulation and are much larger than either the radiation source or the tally volumes located in the skin. The targets (tallies) of the radiation were modelled as cylinders located inside the cube of skin, with one of the end sides facing the surface of the skin.

The main type of tally used in the work described in this report, known as *f8, recorded the energy deposition in units of MeV. Equation 1 was used to convert the deposited energy into a dose rate in skin, DR_{skin}, with units of Gy h^{-1} per Bq:

$$DR_{skin} = \frac{E_{*f8}}{m} C_{Gy} S_{hr} \quad (1)$$

Where E_{*f8} is the deposited energy given by the tally output of MCNP (MeV/s), m is the mass of the tally cell (kg), C_{Gy} is a factor that converts energy deposited in a unit mass into absorbed dose (1.60 10^{-13} Gy per MeV kg^{-1}), and S_{hr} is the number of seconds in one hour (3600).

This absorbed dose rate is to be used to estimate the potential for tissue reactions in the tally area in the skin and not to give an estimate of the risk of cancer induction. The contribution from skin exposure to effective dose is calculated by dividing the energy deposited by the mass of the skin over the whole body and multiplying by the tissue weighting factor for the skin (0.01) (ICRP (1991a), ICRP (2007)).

The tally cylinders were stacked at different depths so that the dose rates estimated using MCNP could be associated with skin at a particular depth (see Figure 2).

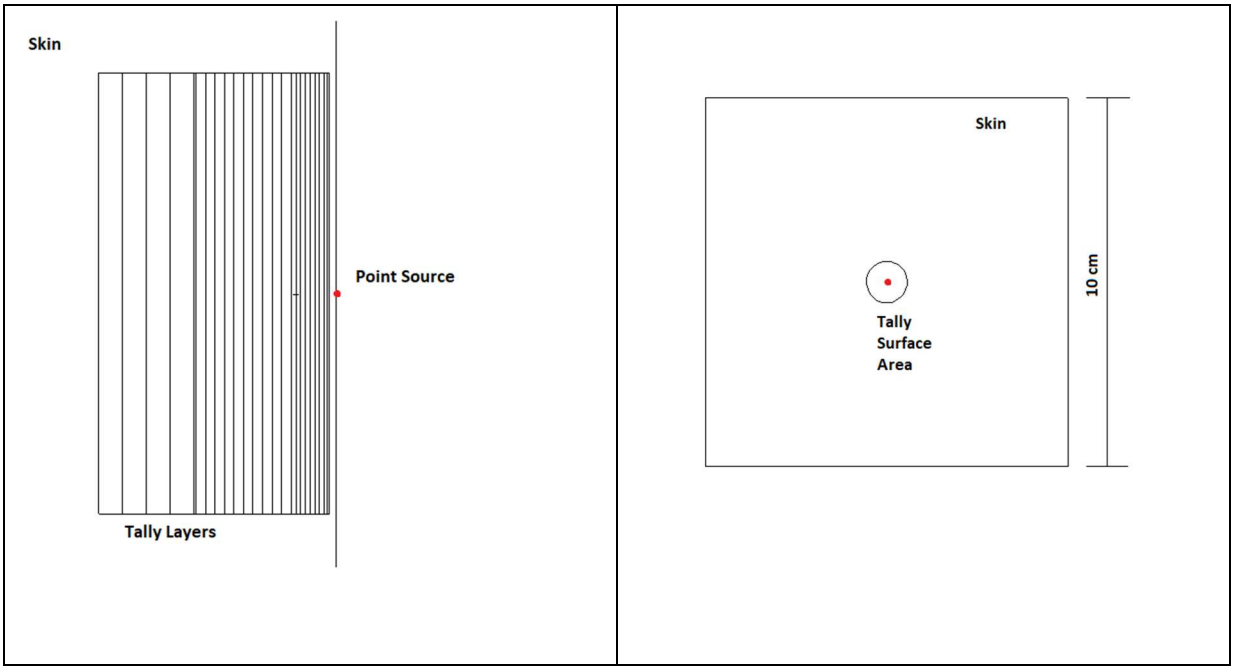

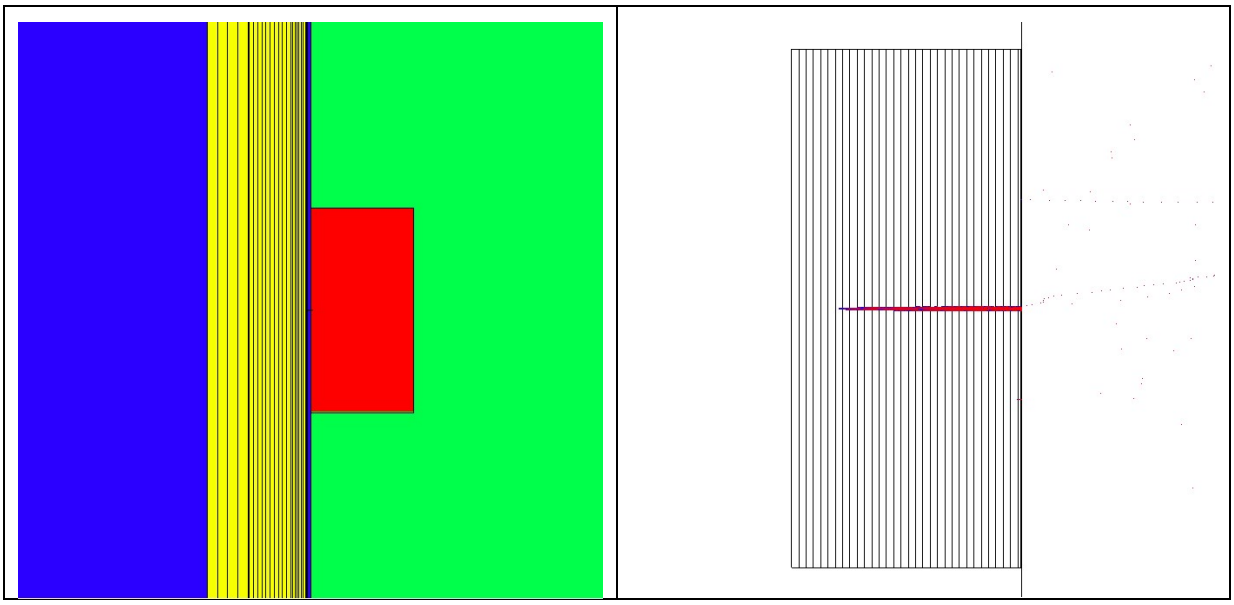

Figure 2: Model of the skin used in the calculations. Top left: the red dot shows the location of the point source above the photon/electron tally cells and the rest of the skin. Top right: 1 cm^2 circular tally area within 10 by 10 cm of skin from above. Bottom left: false colour picture of object (red) on surface of skin (blue) and tally layers (yellow). Bottom right: blue and red dots show collisions caused by alpha and secondary particles into tally cells for alpha particle runs. Note that the dimensions of all the pictures have been distorted to more clearly show the tally cells.

Two different surface areas for the cylinder were chosen to match those used in experiments (1.1 mm^2) (e.g. Kaurin et al, 1997) (ICRP, 1991b) and ICRP recommendations for skin dose calculations (1 cm^2).

When using MCNP to estimate the dose rate in skin from exposure to gamma and beta radiation, the depths of the sections in the cylinder (ie the target cells in skin) were chosen to allow greater resolution in the region of skin where most of the energy from the beta radiation was expected to be deposited. Conversely, larger cells were used at greater depths where accuracy of estimated dose rate with depth was of lesser concern due to beta radiation not being expected to penetrate to those depths in significant quantities. The target sections were 5 μm thick between 15 and 25 μm depth, 10 μm thick between 25 and 95 μm, 20 μm thick between 95 and 295 μm, and 50 μm thick between 300 and 500 μm. Note that there is a non-tally cell of 5 μm between the bottom of the third section (295 μm) and the top of the fourth one (300 μm). This was done to start the next tally cell at 300 μm which was considered better for comparisons with other work.

When estimating the dose rate in skin from exposure to alpha particles, a different set of target depths were used as the penetration of alpha particles into skin is markedly different to that of beta particles. For alpha particles the target sections were 1 μm thick between the surface and 1 μm depth, 2 μm thick between 1 μm and 63 μm and 4 μm thick between 63 μm and 75 μm recognising that few alpha particles would penetrate to such depths and hence greater accuracy in estimated dose rate was not required.

2.1 Methodology for Monte Carlo simulations of point sources

For the calculation of dose rates for gamma and beta radiation, the sources of radiation on the skin were firstly modelled in MCNP as point sources located on the surface of the skin. Radiation emitted by the source was modelled as being either monoenergetic or as a radionuclide specific emission spectrum.

The energies of monoenergetic gamma rays and beta particles were selected as step values between the minimum and maximum of the range of energies typically emitted by radionuclides. In addition, dose rates were calculated for a gamma ray with an energy of 662 keV emitted by ^{137m}Ba. The gamma ray energies used in the assessment were: 10 keV, 20 keV, 30 keV, 50 keV, 70 keV, 100 keV, 125 keV, 150 keV, 200 keV, 300 keV, 662 keV, 1.5 MeV, 2 MeV, 2.5 MeV, 3 MeV.

The energies of beta particles included in the assessment were: 70 keV, 100 keV, 125 keV, 150 keV, 200 keV, 300 keV, 500 keV, 700 keV. 1 MeV, 1.5 MeV, 2 MeV, 2.5 MeV, 3 MeV.

Alpha radiation is notable for its low penetration, and it is often assumed that it does not deposit energy within the basal cells of the skin. For this reason, the effect of being irradiated by alpha radiation is commonly not considered when assessing the risks posed by a source of radiation located outside of the body. However, ICRP Publication 116 (ICRP 2010) recognised that very high energy alpha particles may penetrate the skin and deposit their energy in the basal cells. ICRP Publication 116 gave a lower limit of 6.5 MeV for the energy of an alpha particle able to penetrate down to an assumed depth of the basal cells of 50 µm. However, this depth within the population varies as a function of age.

In ICRP Publication 107 (ICRP, 2008), there are 43 radionuclides that emit alpha particles with energies greater than 6.5 MeV. These radionuclides are generally obscure or short-lived; however, some are progeny of more common radionuclides, like ^{218}At and ^{214}Po in the ^{238}U decay chain or ^{212}Po and ^{216}Po in the ^{232}Th decay chain, and therefore have the potential to be present on objects in the environment that could end up attached to the skin and therefore pose a risk to health that is not normally assessed.

To investigate the relationship between alpha particle energy and dose rate in skin at various skin depths, the dose rate from exposure to alpha particles with the following energies were calculated:

4 MeV, 5.1 MeV (energy of alpha particles emitted by ^{239}Pu), 5.3 MeV, 5.5 MeV (energy of alpha particles emitted by ^{238}Pu and ^{241}Am), 6 MeV, 6.5 MeV, 7 MeV, 7.5 MeV, 8 MeV

Real world exposure to radionuclides on small objects involve radiation possessing a range of energies and radiation types. For example, both ^{90}Sr and ^{137}Cs are commonly found on discrete radioactive objects in the environment in the UK, and these radionuclides are in secular equilibrium with their respective radioactive progeny. Strontium-90 together with its progeny, ^{90}Y, emit beta rays (mean energy 0.196 and 0.933 MeV, respectively) and low

intensity gamma and X rays. Caesium-137 together with its progeny, ^{137m}Ba, emit beta radiation (mean energy 0.188 MeV), a conversion electron, a 0.662 MeV gamma ray and a series of X rays. Other radionuclides found on objects in the environment in the UK are ^{241}Am and members of the radioactive decay chain headed by ^{226}Ra. These radionuclides emit beta and gamma rays, as well as alpha particles.

Thus, following the work with monoenergetic radiations, dose rates from actual emission spectra of some radionuclides were also calculated. The radionuclides selected for this part of the study were ^{90}Sr/^{90}Y, ^{137}Cs/^{137m}Ba, ^{241}Am/^{237}Np and the ^{226}Ra decay chain, since these radionuclides are commonly detected on radioactive objects that have been collected in the UK.

2.2 Methodology for the calculation of absorbed dose for different object shapes and material composition

In reality, the radiation source representing a radioactively contaminated object would not be a mathematical point but would have a volume and a composition with radionuclides being concentrated or dispersed within or on the object. Such features of the source are important as radiation emitted from radionuclides not located close to where the object is in contact with the skin may be absorbed by the object itself, something not accounted for if the source is modelled as a point. Consequently, additional MCNP runs were performed to investigate the impact of an object shape on the dose rate in skin. As real-world objects have complex irregular shapes which are difficult to reproduce in MCNP, all objects were modelled as cylinders. Initially, these cylinders had a radius and height of 500 μm and were made of either iron, sand, or graphite. These materials were chosen as they are similar to the composition of objects that have been found in the environment on beaches near to the Dounreay and Sellafield nuclear licensed sites (Dennis et al, 2007). The effect of changing the density of the object was also investigated by performing calculations with the object made of sand having densities of 1.7 g cm^{-3} and 3 g cm^{-3}. The elemental compositions of objects used in this study were taken from McConn et al (2011) and are given in Table 1, together with the skin elemental composition taken from ICRP Publication 110 (ICRP, 2009).

Table 1 Elemental composition (% weight) and density (g cm^{-3}) of object materials, skin, and air

Element	Skin	Air	Iron	Graphite	Sand	Dense sand
Hydrogen	10.0				0.7833	0.7833
Boron				0.0001		
Carbon	19.9	0.0124		99.9999	0.336	0.336
Nitrogen	4.2	75.5268				

Element	Skin	Air	Iron	Graphite	Sand	Dense sand
Oxygen	65.0	23.1781			53.6153	53.6153
Sodium	0.2				1.7063	1.7063
Aluminium					3.4401	3.4401
Silicon					36.5067	36.5067
Phosphorus	0.1					
Sulphur	0.2					
Chlorine	0.3					
Argon		1.2827				
Potassium	0.1				1.1622	1.1622
Calcium					1.1212	1.1212
Iron			100		1.3289	1.3289
Density (g cm^{-3})	1.09	0.001205	7.874	1.7	1.7	3.0

The effect of changing the object's thickness on the dose rate at different skin depths was investigated by running MCNP using a series of objects with thicknesses greater or smaller than the initial value of 500 µm. As the object's thickness is already small in relation to the distance a gamma ray can travel, changing its thickness will not result in a significant change in the dose rate in skin for these radiations. Therefore, these calculations were performed only for alpha and beta particles. To ensure there was some penetration into the skin, ^{214}Po was selected as the alpha source because it emits alpha particles with an energy of 7.8 MeV and is present in the ^{238}U decay chain. A 0.24 MeV monoenergetic electron source was also used. The distribution of the radiation source in the object was investigated, considering contamination of the surface of the object, or spread evenly within.

3 Results of the calculation of absorbed doses

3.1 Results for photon point sources

For both tally area sizes, the absorbed dose rate to the skin decreased logarithmically with depth for photons with energies below 0.150 MeV. As shown in Figure 3, photons with the lowest energy (0.01 MeV) were found to produce the highest absorbed dose rates at all depths of the skin. At these low energies, the photoelectric effect dominates the photon's interaction with matter and the absorption is greatest when the photon energy matches that of the binding energies of atoms in the skin. Additional graphs of the absorbed dose rate versus skin depth for a range of photon source energies can be found in appendix A.

Figure 4 shows that for photons with energies above about 0.2 MeV, the dose rate changes from a logarithmic decrease with increasing skin depth to a logarithmic increase. It is also noted that, above photon energies that lie somewhere between 0.3 and 1 MeV, the dose rate decreases with photon energy. This changing behaviour is probably due to Compton scattering (the scattering of photons by electrons, reducing the photon's energy) being more important for intermediate gamma-ray energies, while electron-positron pair production becomes more important for photons with energies above 1.5 MeV (Cooper et al, 2003).

The very low energy photons (~ 0.01 MeV) give rise to highest absorbed dose rates because they interact more with tissue. However, absorbed dose rates from electron sources of the same energy are higher.

The effect on the energy deposited of different target volumes was assessed by running MCNP for two tally volumes defined by a surface area of either 1.1 mm^2 or 1 cm^2. The ratio of energy deposited in these target cells and absorbed dose rates for photons with different energies is shown in Figure 5 and Figure 6. Out of the two tally volumes, the one defined by a surface area of 1 cm^2 had more energy deposited within it. This is because, as photons travel through the tally volume, they are increasingly scattered from their original path but, as the tally volume increases, a greater fraction of these scattered photons are still absorbed in the target volume.

While more photon energy is absorbed in the larger tally volume, the absorbed dose rate in the 1.1 mm^2 tally volume is much higher, by 2 orders of magnitude, compared to that in the 1 cm^2 tally volume; this is shown in Figure 6. The difference in the ratio of absorbed dose rates compared to absorbed energies between the two tally volumes is due to the ratio of the tissue masses being much greater than the ratio between the energy being deposited. Additional graphs showing the difference in absorbed dose rates are in appendix A, Figure 23 to Figure 26.

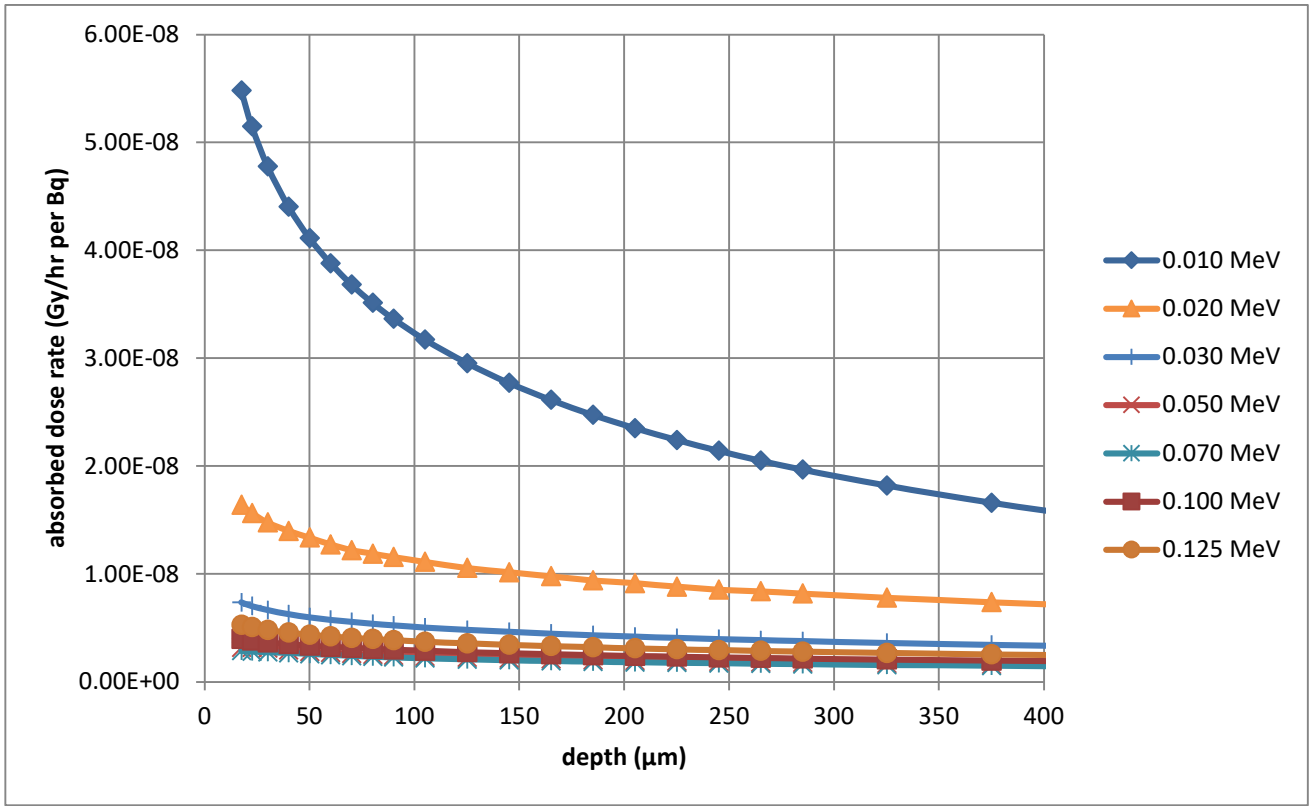

Figure 3: Absorbed dose rates in 1 cm² area tally from low energy, monoenergetic photons

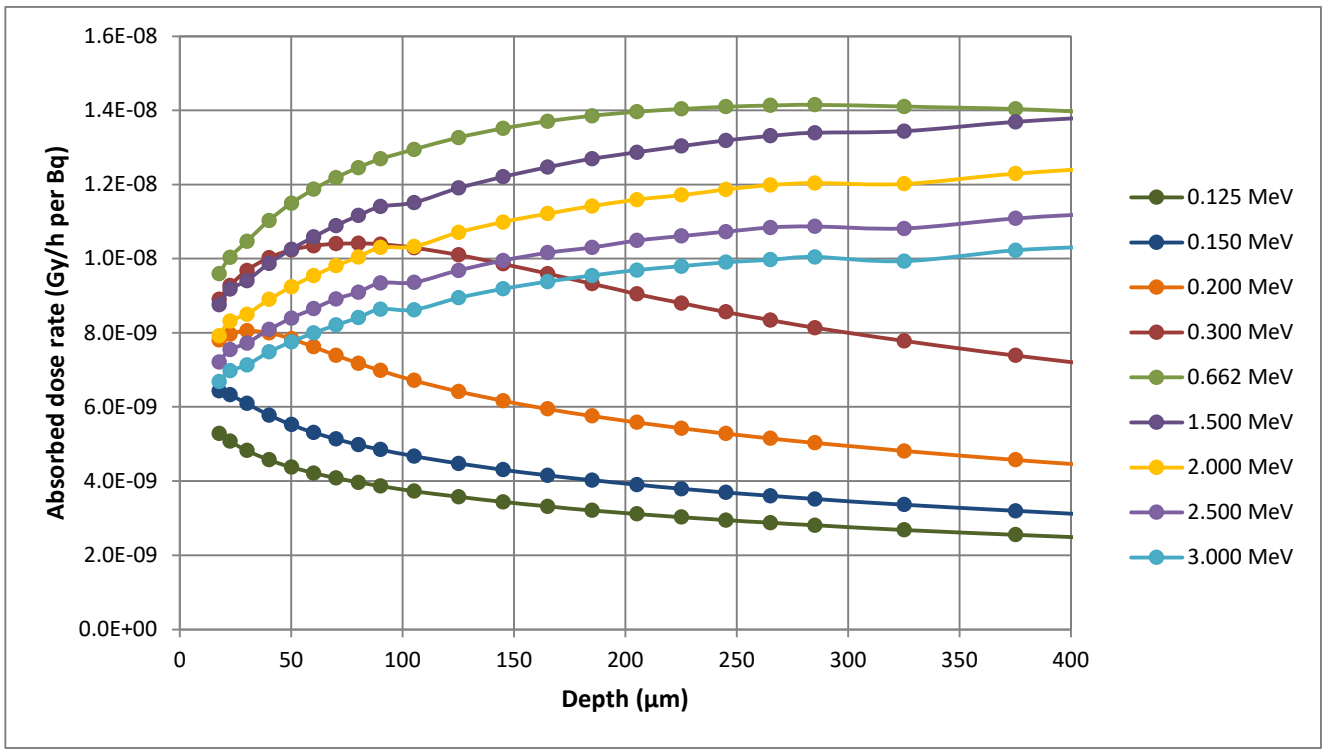

Figure 4: Absorbed dose rates in 1 cm² area tallies at various depths from high energy, monoenergetic photon sources. The dose rates include the effect of secondary charged particles build-up

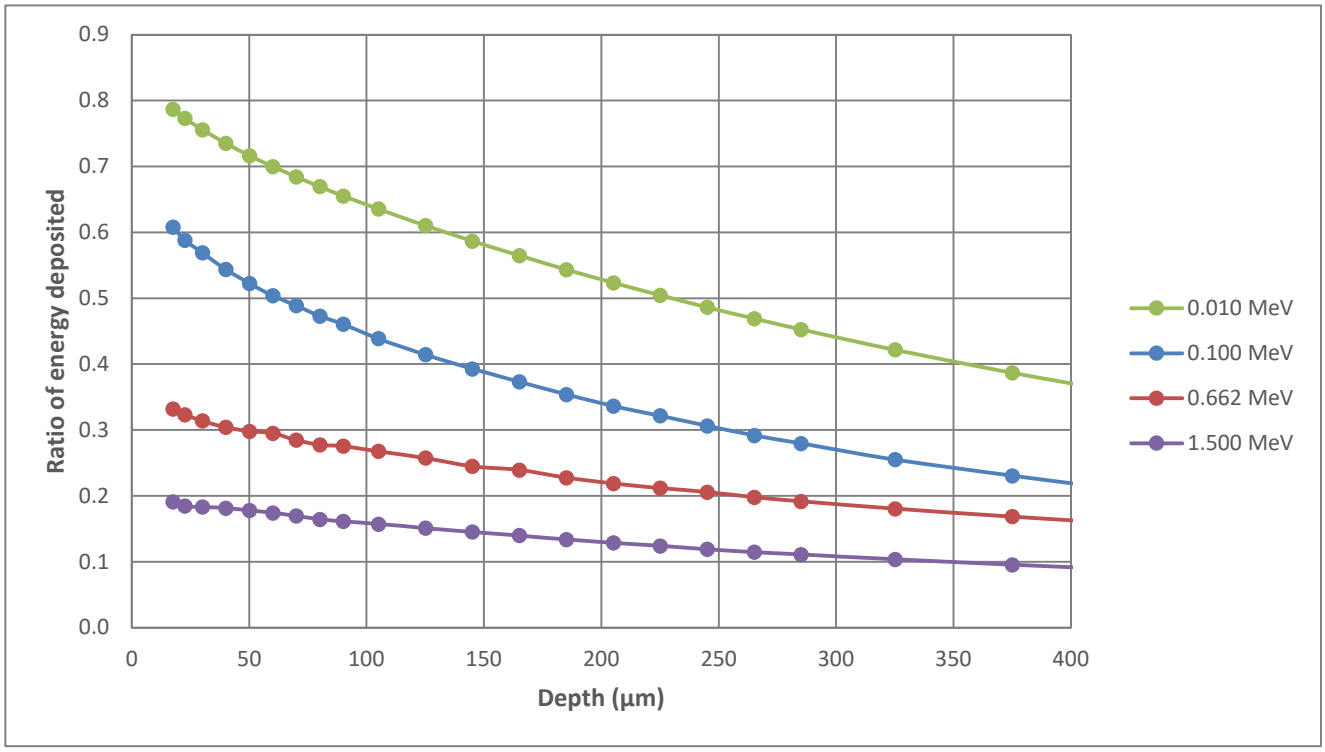

Figure 5: Ratio of energy deposited by photons between the 1.1 mm² and 1 cm² area tallies at different depths

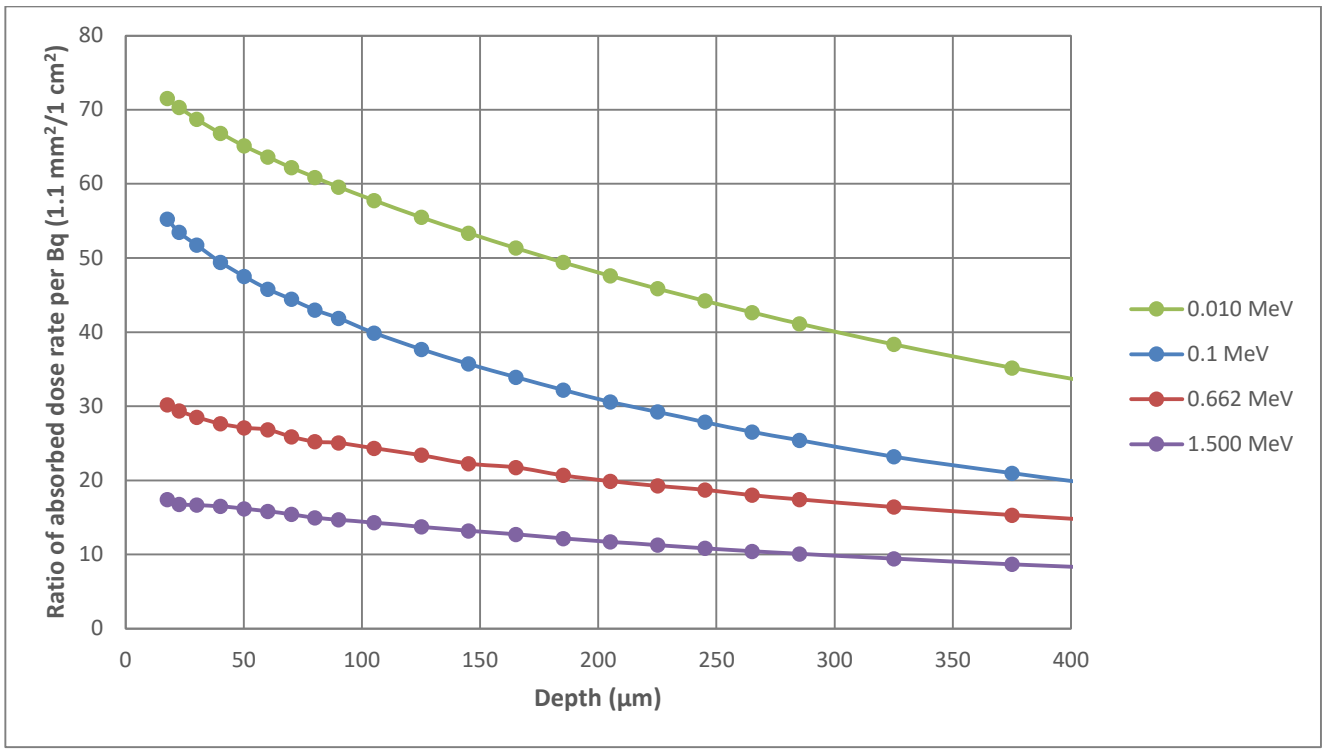

Figure 6: Ratio of absorbed dose rate from photon sources between the 1.1 mm² and 1 cm² area tallies at different depths

3.2 Results for electron point sources

Shown in Figure 7 (also in appendix A, Figure 27 to Figure 31) is the absorbed dose rate versus skin depth for different electron energies. The profiles of the absorbed dose rate with depth for electron energies less than 0.3 MeV have relatively high dose rates close to the surface followed by a gradual decrease in the dose rates at deeper layers within the skin. The depth at which this change in behaviour occurs depends on the source energy. Above 0.3 MeV there is only a gradual decrease in the absorbed dose rate versus depth. By analysing the MCNP results, it is surmised that the first regime relates to the penetration depth of the primary electrons, while the second regime is a result of energy being deposited by secondary photons.

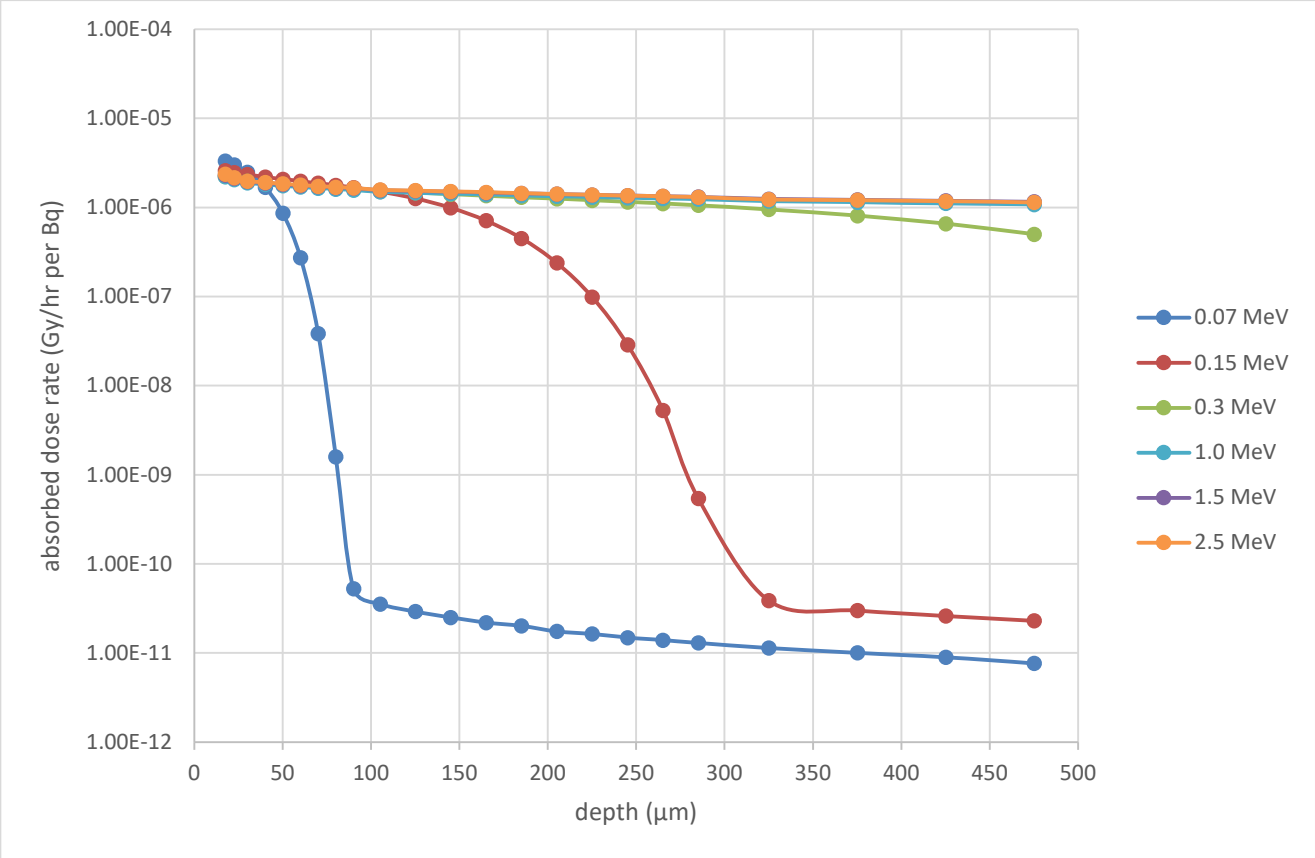

Figure 7: Absorbed dose rates in the skin (1 cm^2 tallies) for monoenergetic electron sources

Figure 8 shows the ratio in energy deposited in the MCNP (1.1 mm^2 and 1 cm^2) tallies by electrons emitted by a source of radiation in contact with the skin. For electrons with energies up to 0.15 MeV, there is little difference between the energy deposited within the two tally surface areas to skin depths of under 150 µm. However, at greater depths, around 300 µm for 0.1 MeV electrons, about 40% more energy is deposited in the 1 cm^2 tallies when compared to the 1.1 mm^2 tallies. For higher energy electrons, the ratio of energy deposited between the two volumes follows a logarithmic decline, with less energy being deposited in the 1.1 mm^2 tallies compared to the 1 cm^2 tallies. The reason why less energy is deposited in

the 1.1 mm^2 tally surface area is that some of the electrons that enter the skin are scattered and leave the tally volume prior to depositing all their energy. This process is less significant for the larger tally volume as the scattered radiation is more likely to be incident on the larger 1 cm^2 surface area tallies and less likely to travel out of the larger volume, leading to more energy deposition in that tally. The difference is smaller for lower energy electrons and at shallower depths as the stopping power of skin increases as the electron slows down.

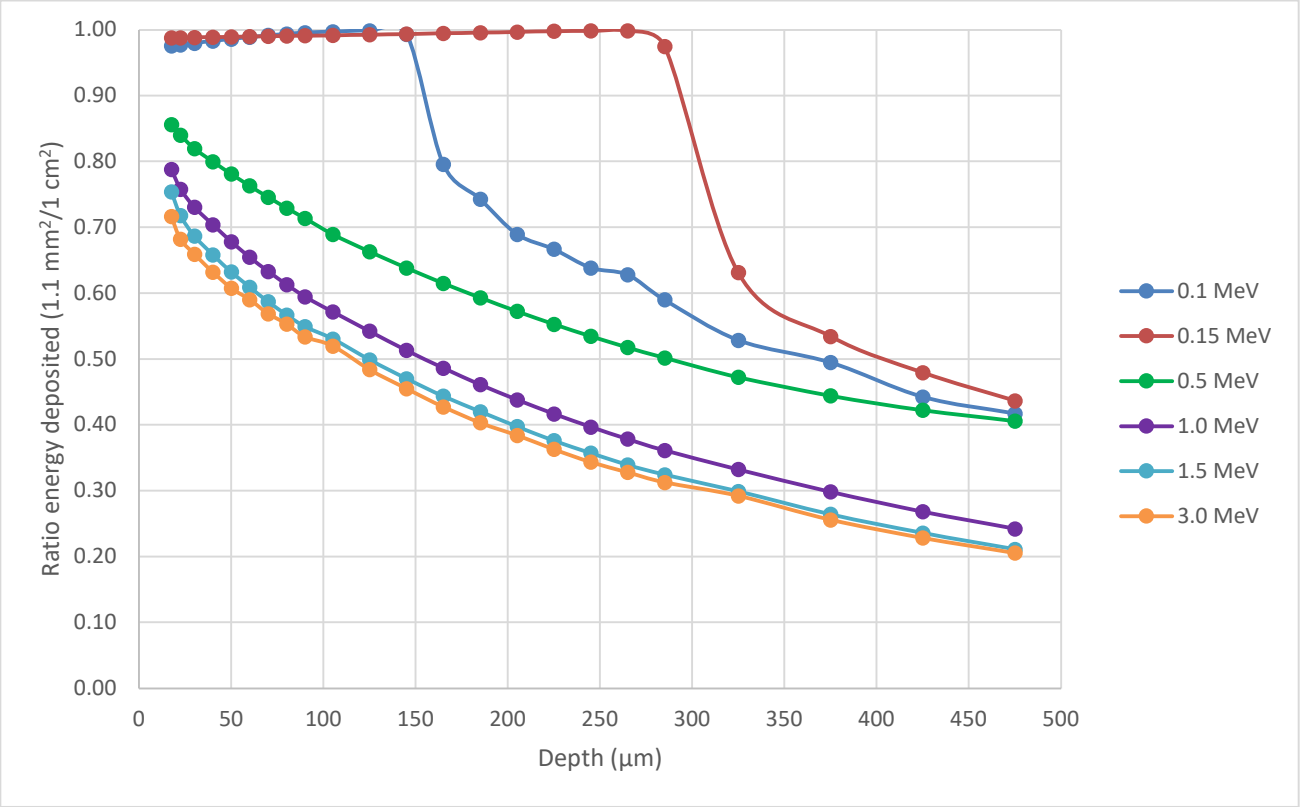

Figure 8: Variation with skin depth of the ratio of energy deposited between the two tally sizes (1.1 mm^2 and 1 cm^2 surface areas) for monoenergetic electrons

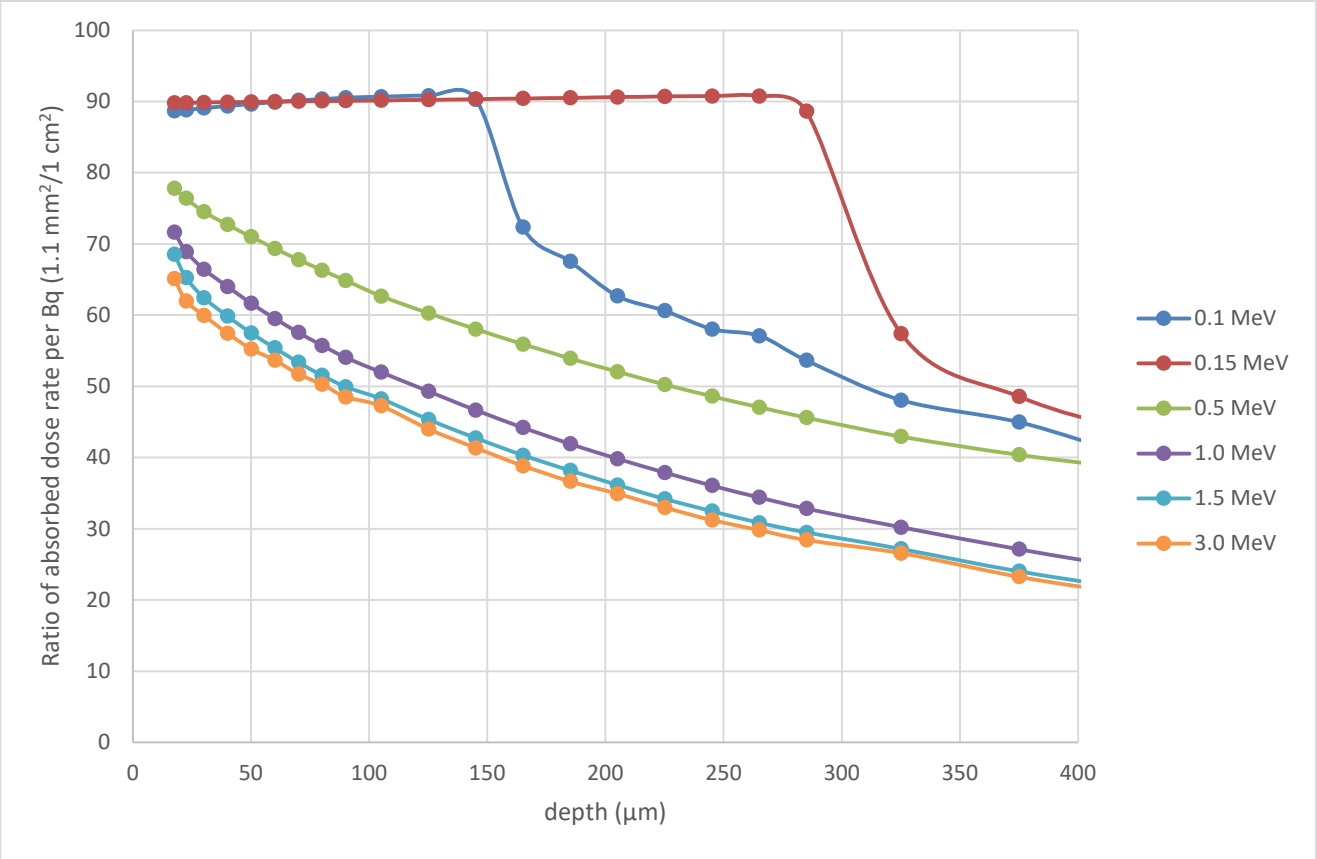

Figure 9: Variation with skin depth of the ratio of absorbed dose rate between the two tally sizes (1.1 mm^2 and 1 cm^2 surface areas) for monoenergetic electrons

3.3 Results for alpha point sources

Figure 10 shows the variation of the absorbed dose rate with skin depth for alpha particles emitted by a point source with energies ranging between 4 and 8 MeV. As expected, due to the large mass and electrostatic charge of alpha particles, their ability to penetrate the skin is significantly lower than that for photon and electron radiations. Figure 10 shows that only alpha particles with energies greater than 6.5 MeV can penetrate the skin to a depth of 50 µm, the lower end of the range recommended by ICRP for assessing radiological risk. It was also estimated that alpha particles of at least 4 MeV have the potential to penetrate the skin to depths of around 20 µm, the minimum thickness of epidermis likely to be present on humans, while alpha particles with energies greater than 8 MeV were estimated to have the potential to penetrate the skin to depths of around 70 µm, well within the range where radiosensitive cells are considered to lie (ICRP, 2010). However, for the alpha particles to be able to penetrate so deeply into the skin they require to be emitted within a small angular range from the normal to the skin surface.

For alpha particles, it was found that the energy deposited within the 1 cm^2 and 1.1 mm^2 tallies were nearly identical. This result indicates that there is no significant scattering of alpha particles within the skin or that, even if scattering occurs, the scattered particles lose most of their energy within both tally volumes due to their limited range.

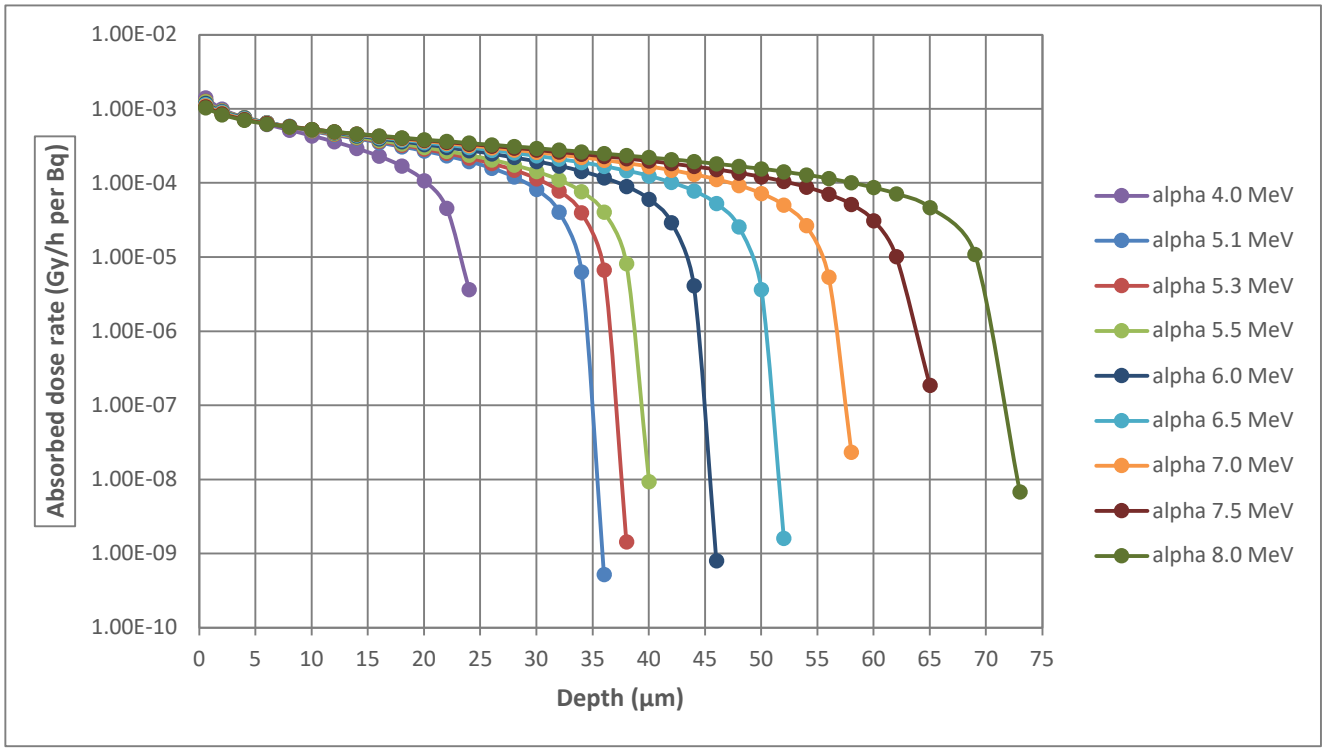

Figure 10: Absorbed dose rate from alpha radiation in a 1 cm^2 area tally at shallow skin depths

3.4 Results for point sources of selected radionuclides

Figure 11 shows the total absorbed dose rate in skin versus skin depth for exposure to radiations emitted by ^{137}Cs/^{137m}Ba. The total dose rate in the skin is dominated by beta radiation from ^{137}Cs, with the dose rate from exposure to the photons emitted by ^{137m}Ba being 130 times lower. This was expected, as the results of the calculation of dose rates for monoenergetic electrons and photons showed that electrons generate higher dose rates, particularly at shallower skin depths.

For ^{90}Sr/^{90}Y (see Figure 12), the total dose rate in skin at all depths is mainly from exposure to the beta emissions of both radionuclides. At skin depths below about 30 to 40 µm, the dose rate to the skin from exposure to beta emission from ^{90}Sr and ^{90}Y are broadly similar. However, as the depth in skin increases, the overall dose rate to the skin is increasingly dependent on exposure to beta radiation from ^{90}Y (β max 2.28 MeV) rather than ^{90}Sr (β max 0.55 MeV) although, at a depth of 200 µm, the ratio of the absorbed dose rate from exposures to beta radiation from these radionuclides is only a factor of two. This result is consistent with the results from the calculations of dose rates to the skin with monoenergetic electrons which showed that primary electrons with higher energy can penetrate further into the skin and produce higher dose rates.

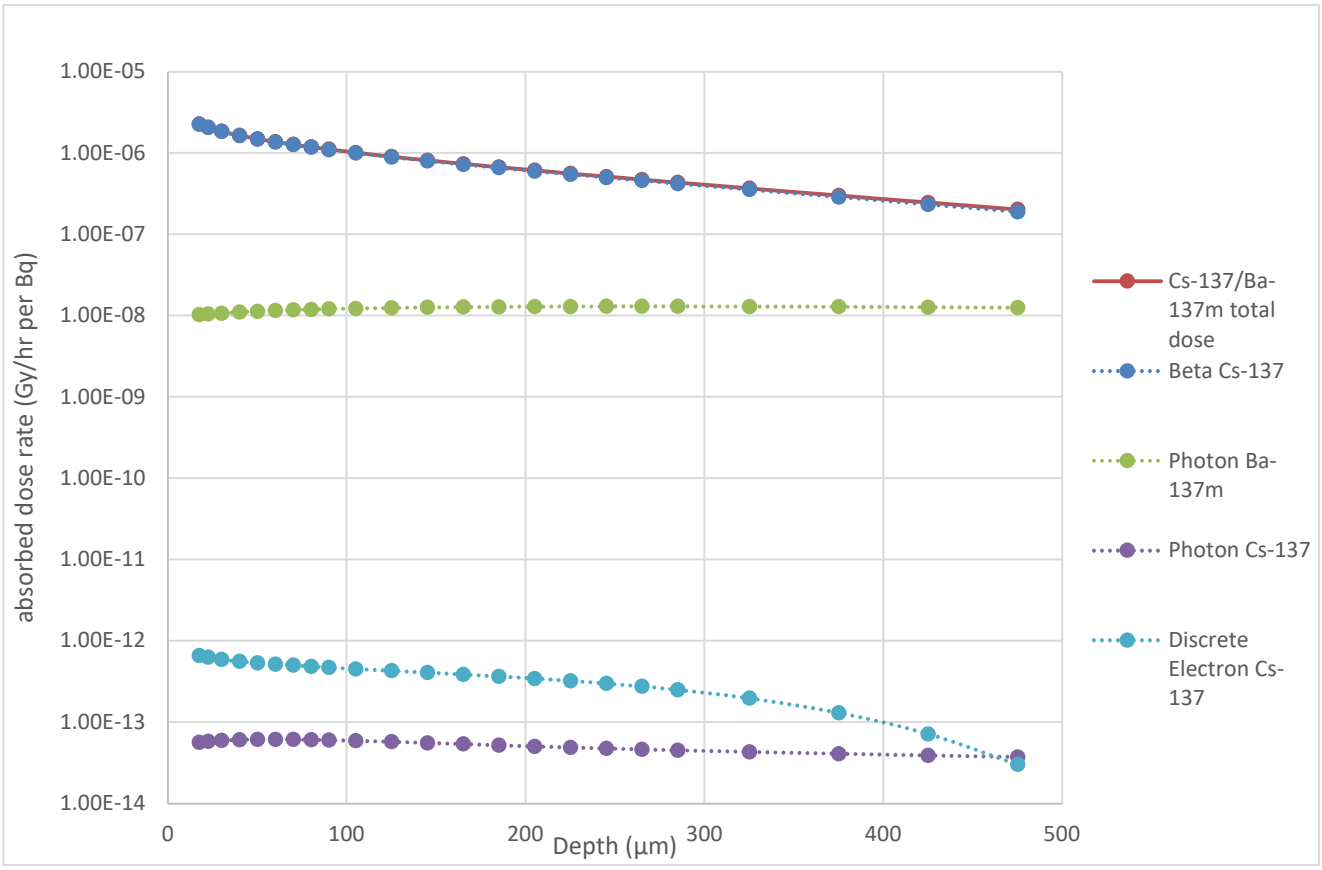

Figure 11: Absorbed dose rate of $^{137}Cs/^{137m}Ba$ in different layers of skin (1 cm^2 tally)

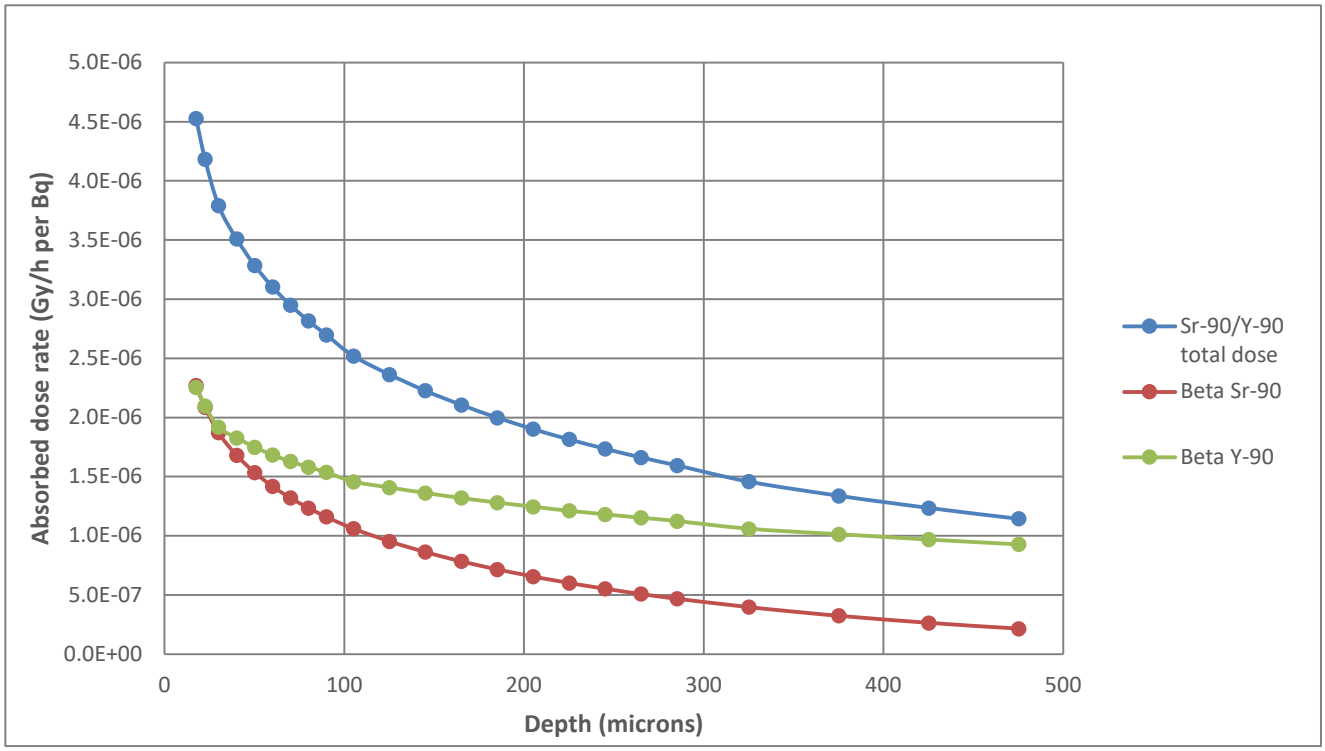

Figure 12: Absorbed dose rate of $^{90}Sr/^{90}Y$ in different layers of skin (1 cm^2 tally). The absorbed dose rate from ^{90}Y photons and ^{90}Y discrete electrons are not shown as much lower

The variation of absorbed dose rate versus skin depth for a source of $^{241}Am/^{237}Np$ is shown in Figure 13. For skin depths less than 50 µm the most significant contribution to the dose rate is from energy deposited by alpha radiation. At skin depths between about 50 and 100 µm, the total dose rate is mainly associated with energy deposited by the discrete electron emissions from ^{237}Np while, at deeper skin depths, the dose rate is mainly due to energy being deposited by gamma radiation emitted by both radionuclides.

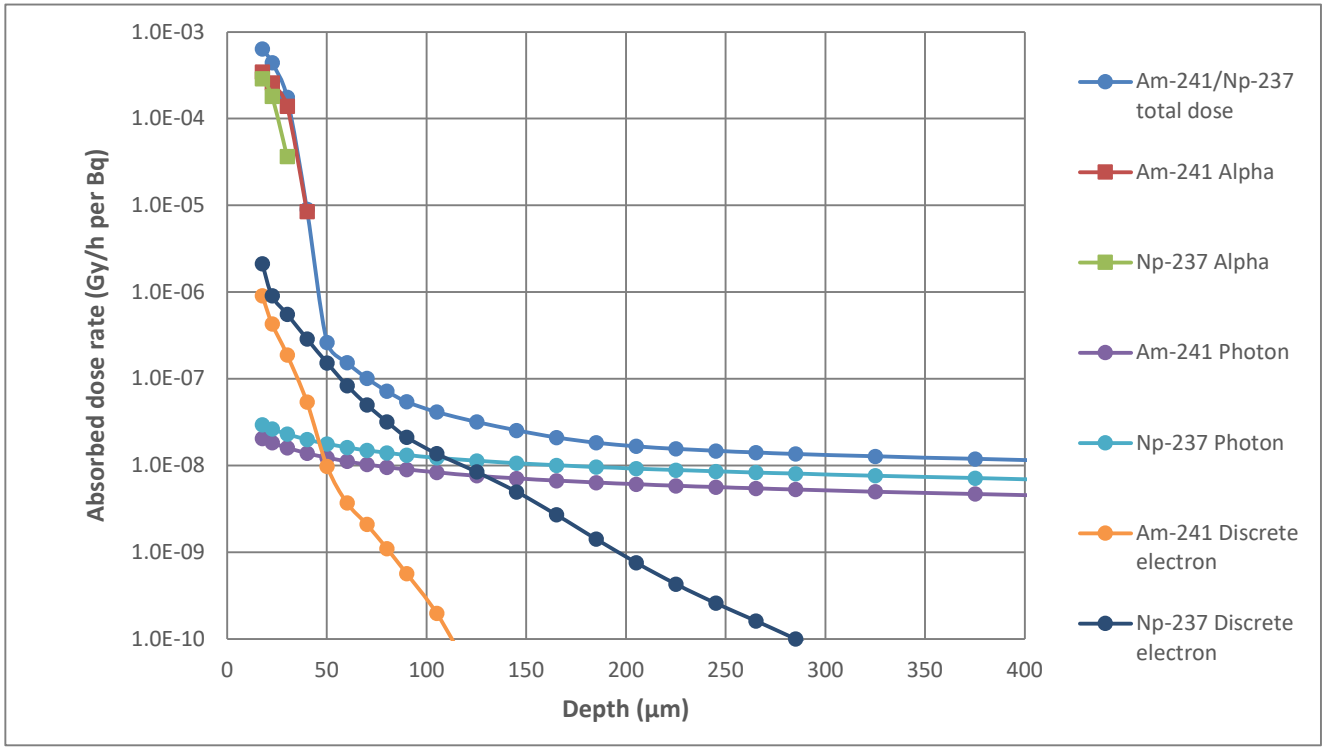

Figure 13: Absorbed dose rate from $^{241}Am/^{237}Np$ in different layers of skin (1 cm^2 tally)

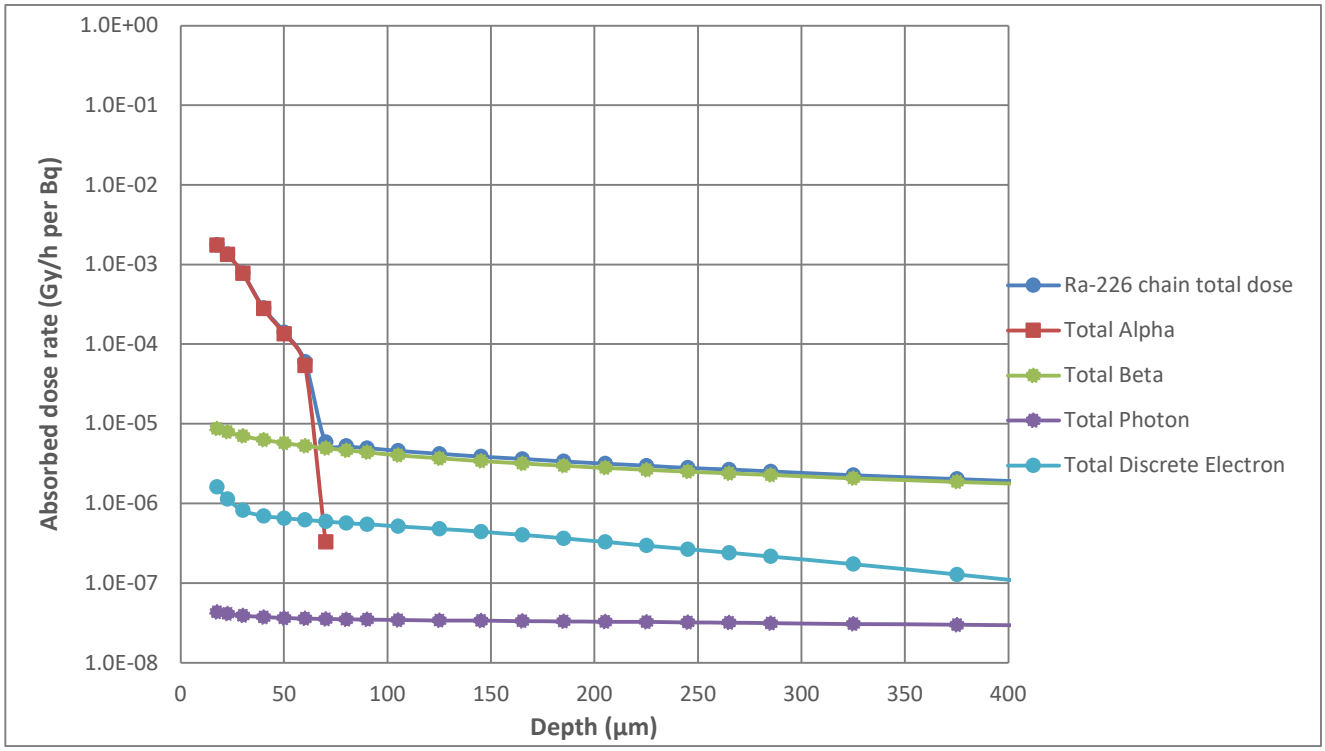

Figure 14: Absorbed dose from ^{226}Ra decay chain in different layers of skin (1 cm^2 tally)

The absorbed dose rate in skin from exposure to radiation emitted by ^{226}Ra and its radioactive progeny is shown in Figure 14. One of the progeny in the radioactive decay of ^{226}Ra is ^{214}Po, a strong alpha emitter which gives the most significant contribution to the dose rate in skin at depths of less than around 60 µm, deeper than the alpha particles penetrate for ^{241}Am. The dose rate to the skin at depths greater than around 60 µm is mainly due to energy being deposited by electrons emitted by the radioactive progeny of ^{226}Ra.

The results of the calculation of absorbed dose rates for ^{226}Ra show that the high energy alpha emitting progeny produce a dose rate of around a factor of 5 higher than from their beta emissions. Therefore, if an assessment omits the alpha emissions of the ^{226}Ra progeny, the result will be a significant underestimation of its absorbed dose rate, though mainly for deterministic tissue reactions at the surface of the skin.

4 Results from realistic radioactive objects

4.1 Variation of absorbed rates from radioactivity on objects of different materials

Figure 15 shows the absorbed dose rates at various depths of skin from 0.3 MeV monoenergetic electrons that are emitted by radionuclides distributed evenly throughout the

cylindrical volume of each object (500 µm radius; 500 µm thick) made of different materials (iron, sand, dense sand and graphite). The closeness of the graphite and sand curves in Figure 15 suggest the main factor affecting the flux of radiation able to leave the object and subsequently deposit energy at a specific depth of skin is the density of the object. As expected, the absorbed dose rate in the skin decreases as the density of an object increases, as more radiation is absorbed within the object. The curves for graphite and sand, both having a density of 1.7 g cm^{-3}, are nearly identical while dense sand (3.0 g cm^{-3}) gives a lower absorbed dose rate. This result is consistent with the observation made by Saito and Jacob (1995) that soil composition is less important for dose rates than density.

Figure 16 shows that for electrons with an initial energy of 1.0 MeV, differences in dose rates between objects of different densities and materials are reduced compared to the dose rates estimated for lower energy electrons. This is due to the higher energy electrons passing more easily through matter and therefore being less affected by smaller variations in the density of an object.

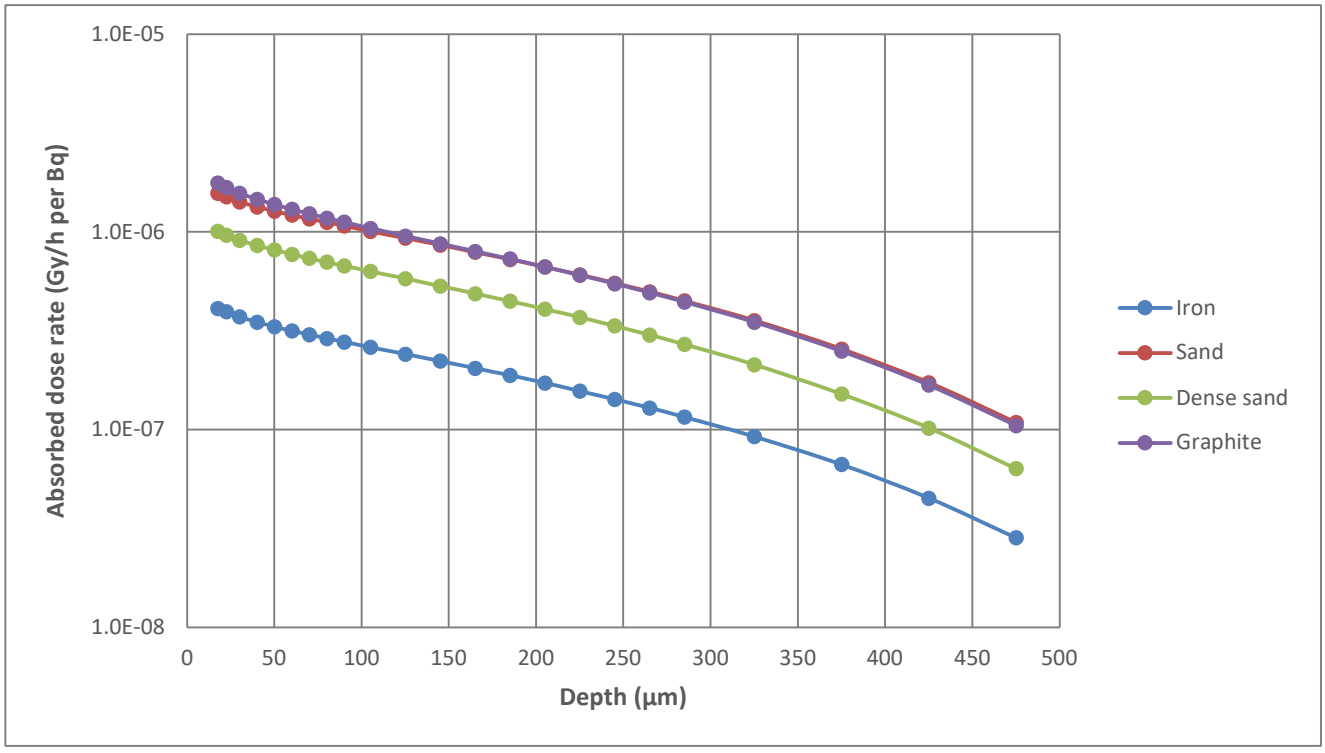

Figure 15: Absorbed dose rate in skin by 0.3 MeV electron source distributed in different small cylindrical objects made of different materials (1 cm^2 tally)

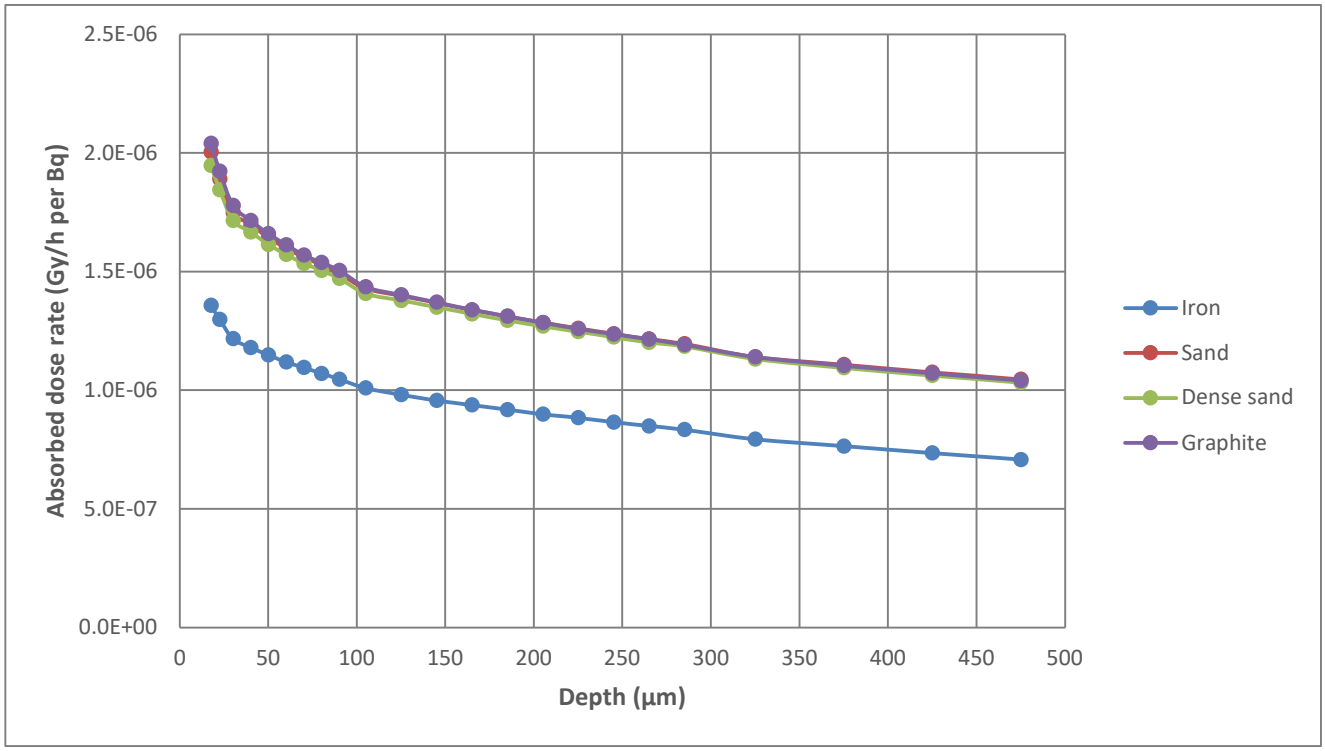

Figure 16: Absorbed dose rate in skin by 1.0 MeV electron source distributed in different small cylindrical objects made of different materials (1 cm^2 area tally). Note the sand, dense sand and graphite data points are close together

The absorbing properties of a cylinder of dense sand with a radius of 500 µm and a thickness of 500 µm (see Table 1) was investigated by comparing the dose rate in skin from such an object containing ^{137}Cs against the dose rate from a ^{137}Cs source distributed on a disk (i.e. no thickness) of the same radius. Figure 17 shows the difference in the absorbed dose rates for these two sources. The figure shows that absorption within the cylinder of dense sand reduces the dose rate in the skin by a factor of about 4 for depths of between a few tens to a few hundreds of micrometres. Objects have been found on Sellafield beach with dimensions of a few hundred micrometres (Oatway et al, 2011). This result shows the importance of the distribution of radioactivity within an object, which is substantially increased if the contamination is all on the side facing the person exposed.

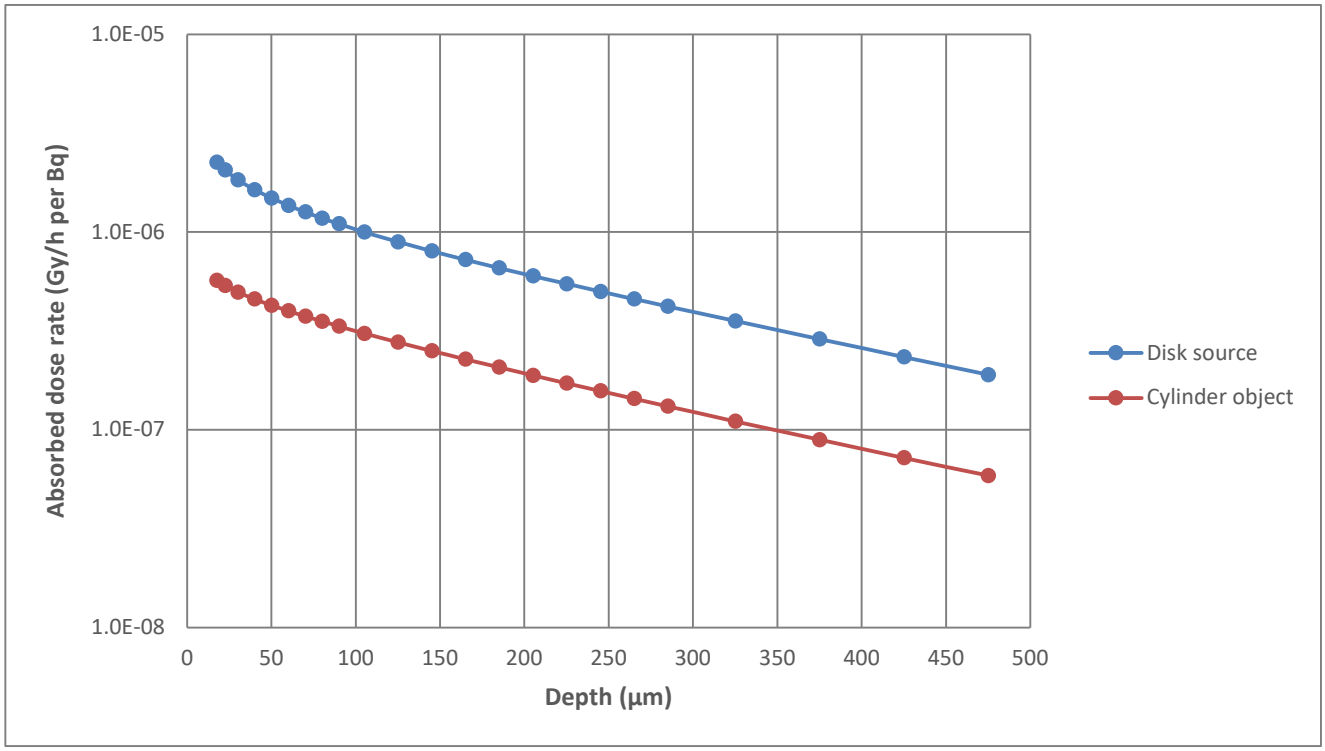

Figure 17: Absorbed dose rate in skin for ^{137}Cs Beta source in a disk and a cylindrical object (1 cm^2 area tally)

4.2 Effect of radionuclide distribution in objects

A ^{214}Po source emitting alpha particles with an energy of 7.8 MeV was used to investigate the effect on the absorbed dose rate of the distribution of radioactivity in a small radioactive object. Figure 18 shows the absorbed dose rate in the skin in tallies with a 1 cm^2 surface area below a source within a 500 µm radius, 500 µm thick iron cylinder. Iron was chosen as its higher density meant that distribution effects on the absorbed dose rates would be greater. When the source is confined to the bottom of the cylinder, next to the skin, the dose rate is approximately a factor of a hundred higher than when the source is on top of the iron cylinder away from the skin. If the radioactivity is distributed throughout the cylinder, with the same total activity, the absorbed dose rate in the skin is about a factor of three higher than if the radioactivity is restricted to the top, though still much lower than when all the radioactivity is next to the skin. The dose rate vs skin depth curve is significantly different compared to that for an alpha point source (see Figure 10) due to the horizontal spread of the source. Figure 19 shows the effect on the absorbed dose rate of the distribution of an electron source with an energy of 0.24 MeV in an iron cylinder. When the source is located only on the bottom surface of the object next to the skin, the dose rate is a factor of 50 higher than when the source is on the top surface of the iron cylinder away from the skin. The variation of the absorbed dose rates with skin depth shows a similar pattern to that generated by that the alpha source but with a smaller difference between different distributions of the source likely due to the penetrating power of electrons.

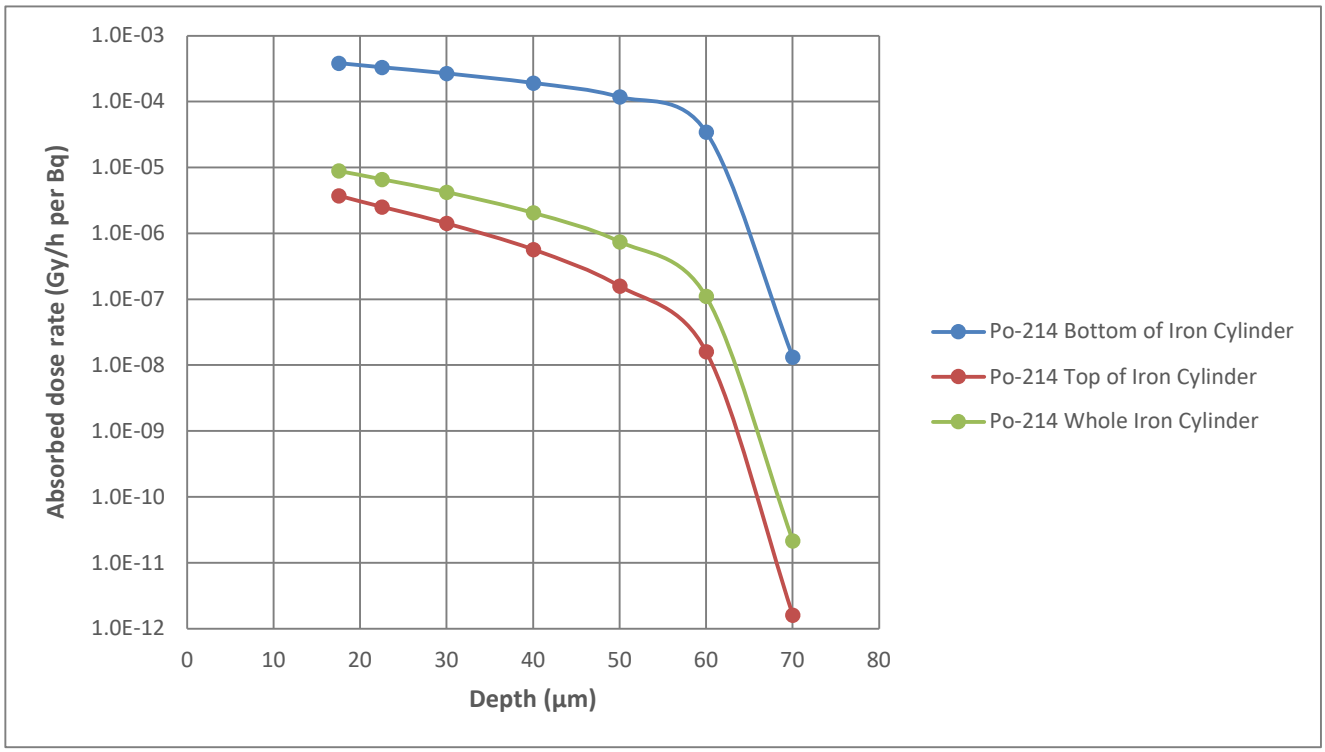

Figure 18: The effect of ^{214}Po source distribution through iron cylinder on absorbed dose rate in skin (1cm^2 area tally)

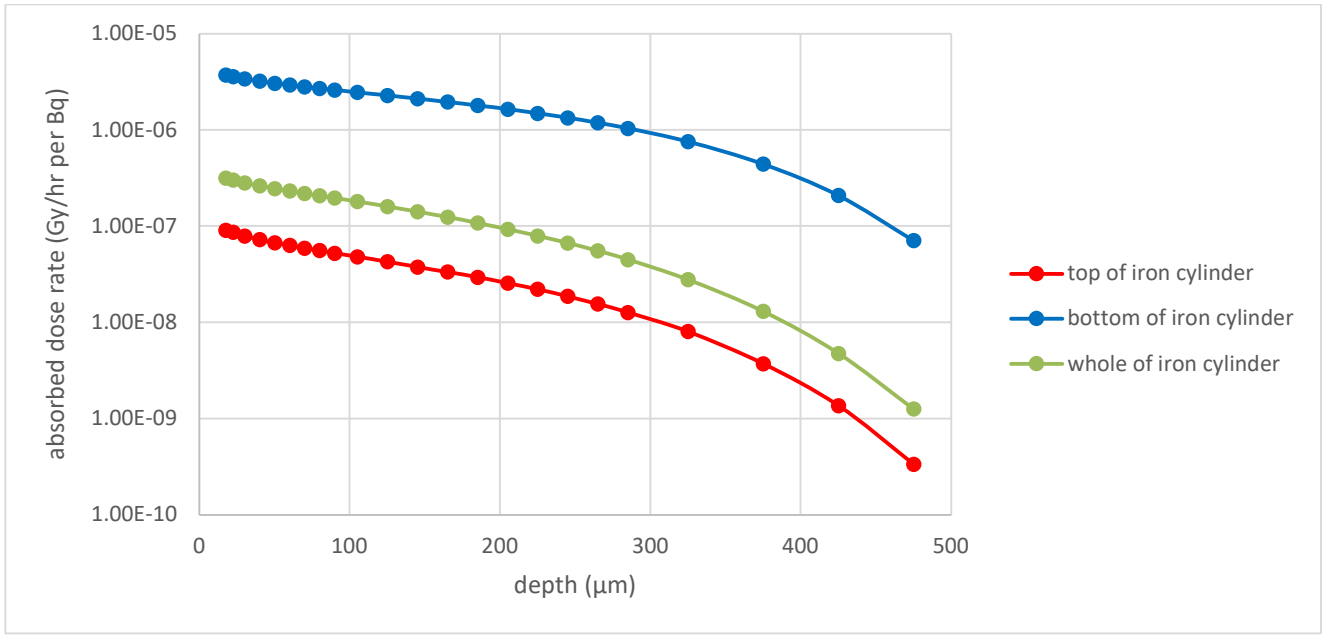

Figure 19: The effect of 0.24 MeV electron source distribution through iron cylinder on absorbed dose rate in skin (1 cm^2 area tally)

To investigate the impact of the thickness of the object on dose rate, a series of MCNP runs was performed for different cylinder heights with an alpha (^{214}Po) or electron (0.24 MeV) source present only on the surface facing away from the skin. The results for the alpha

source are shown in Figure 20. As expected, the absorbed dose rates decrease with the thickness of the object. The reduction in dose rate with the thickness of the object is due to alpha particles starting on the top surface of the object being less able to reach the skin, even via the surrounding air. Objects found near Dounreay have ranged in size from 100 µm to 2 mm (Byrnes et al, 2020). The differences between dose rates generated by radioactivity on objects with different thickness narrow slightly at deeper skin depths, as only alpha particles travelling directly down reach the deeper layers of the skin. Figure 21 shows that for electron sources the absorbed dose in the skin does not reduce to zero at deeper skin depths and the effect of object height is a linear reduction in absorbed dose rate over a range of 125 µm to 750 µm.

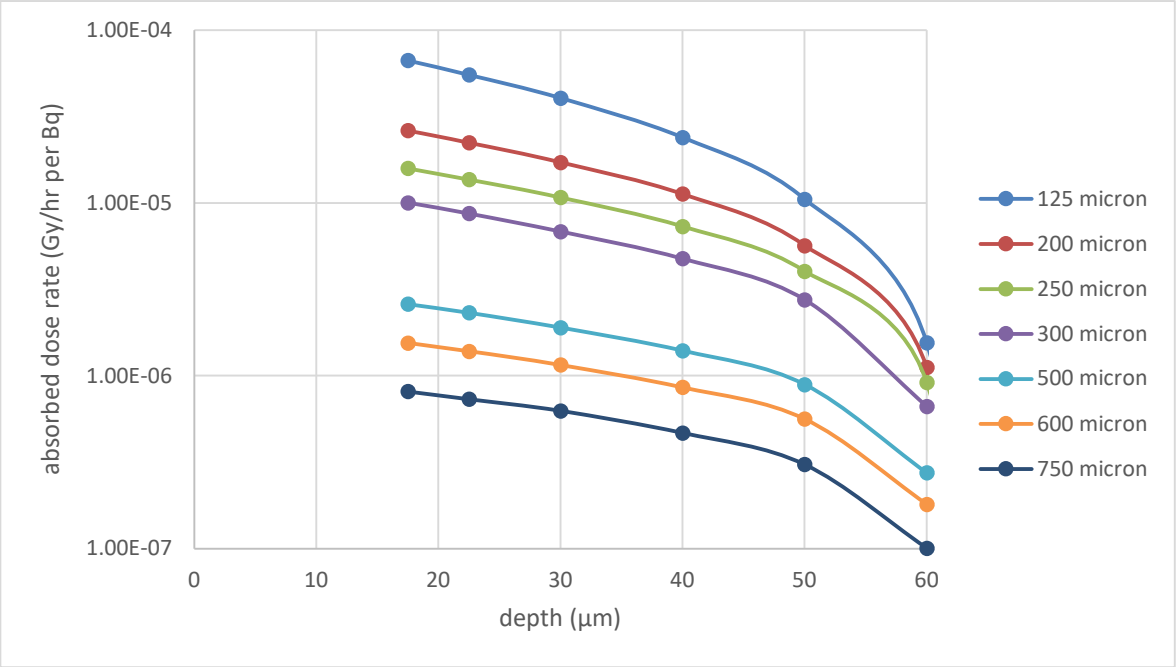

Figure 20: The effect of object height on absorbed dose at different depths in the skin from a ^{214}Po source on the top surface of an iron object (1.1 mm^2 tally area)

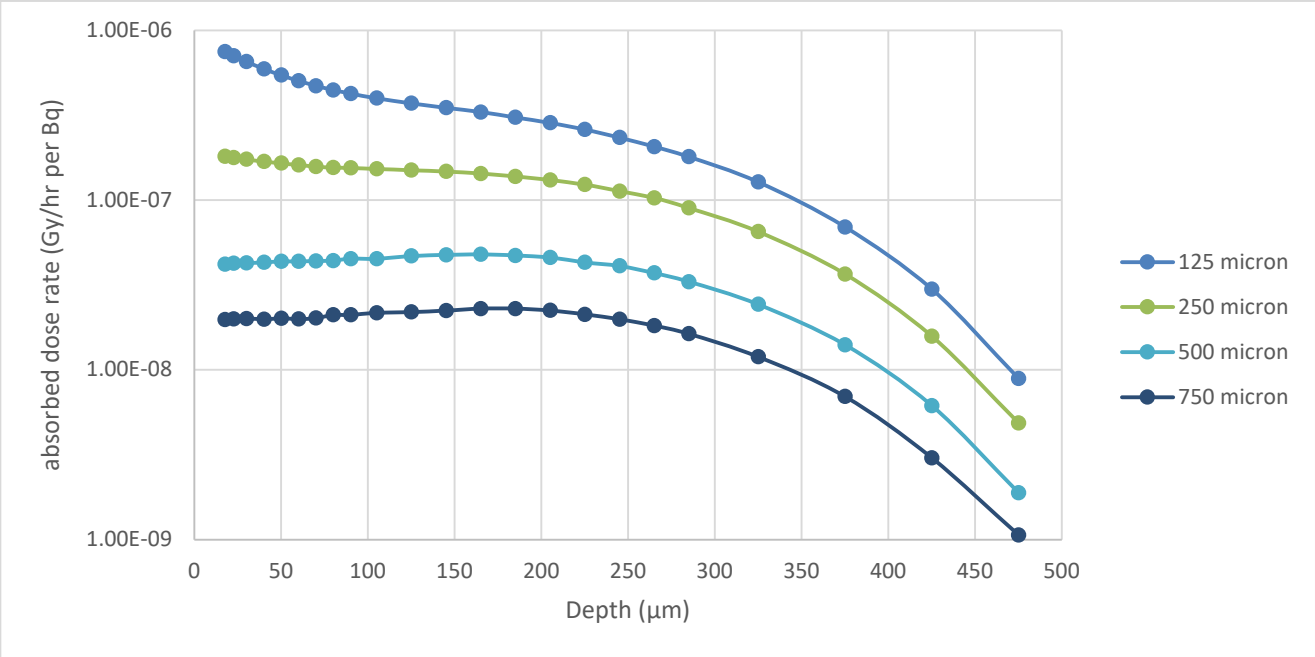

Figure 21: The effect of object height on the absorbed dose at different depths of the skin from a 0.24 MeV electron source on the top surface of an iron object (1.1 mm^2 tally area)

The impact of changing the radius of the source was also investigated. However, the geometry of this simulation makes the results difficult to interpret as it alters how the object covers the tally surfaces. For example, when a simulation is run for an object with a radius of 1 mm, the dose rate recorded is 0, for all but the thinnest objects, for the 1.1 mm^2 tallies as the source object is wider than the tally area, which has a radius of about 0.59 mm. However, a positive dose rate is calculated for the same object when the 1 cm^2 area tallies (radius approximately 5.6 mm) are used, suggesting that the radiation is travelling through the air surrounding the object and not the object itself. If the radioactive object was bigger than the area of the tallies in the skin, radiation travelling from the edge of the source does not enter the tallies and is not recorded in the simulation. This is an artefact of the calculation model because for a real object on a person's skin, a dose would be received irrespective of its size, though perhaps not below where the object is in contact but spread over larger volume of skin.

The simulation with MCNP also showed that when the object area is greater than the tally area, the alpha particles emitted by a ^{214}Po source on the top side of the object could only reach the skin if the thickness of the object is 15 µm or less (see Figure 22) and only reach 50 µm depth in the skin if the thickness of the object is 5 µm or less.

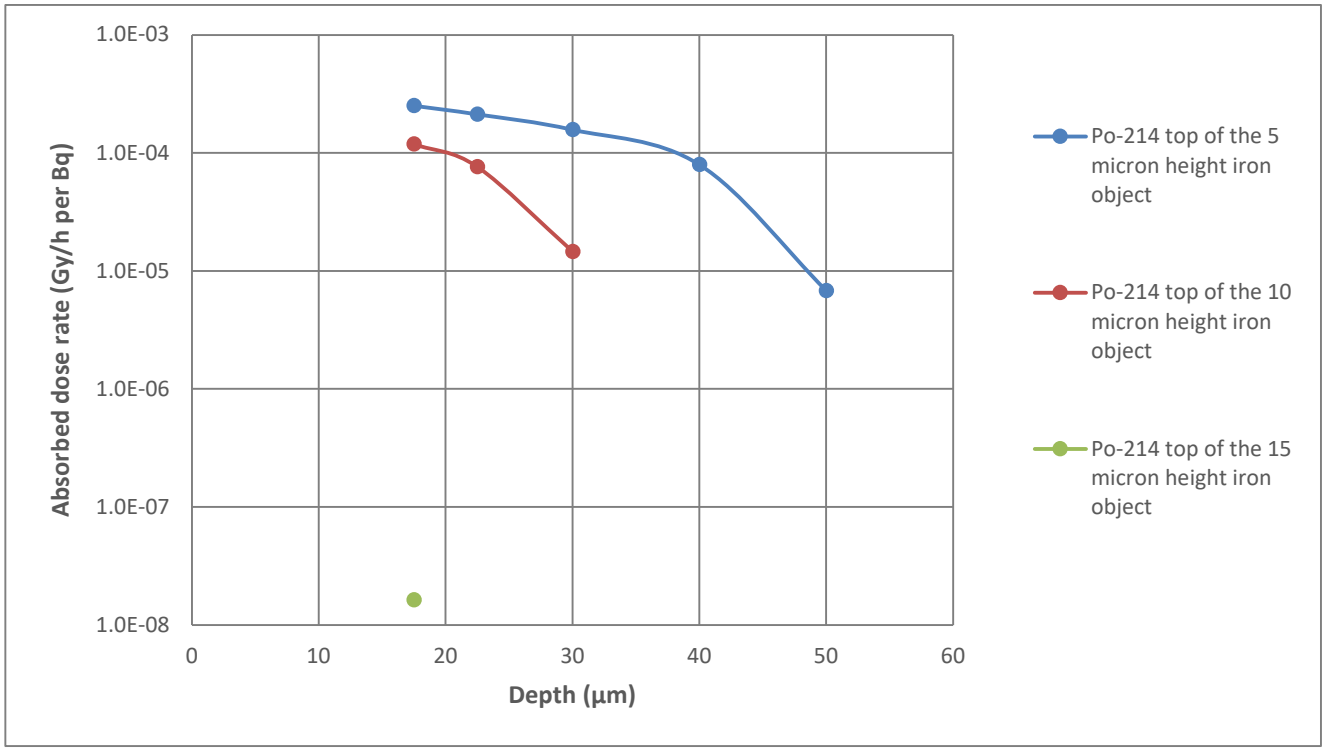

Figure 22: ^{214}Po penetration when object covers tally area (1 cm^2)

5 Conclusions

This report describes a study using a Monte Carlo radiation transport code to estimate absorbed dose rates to skin from irradiation by objects containing radioactivity in contact with the skin. The estimated absorbed dose rates are discussed with respect to how they vary with depth within the skin, in particular at depths where radiosensitive cells may be present, and their dependency on both the energy deposited in the tally and area (therefore mass) of skin tissue within the tally. The simulations performed included irradiation by monoenergetic radiation emitted by photons, electrons, and alpha particles and by radiations emitted by ^{241}Am, ^{137}Cs, ^{90}Sr and ^{226}Ra, which are the radionuclides commonly found on contaminated objects present in the environment in the UK. The study also investigated how the distribution of radioactivity on and within an object affected the dose rate in skin, accounting for self-shielding of radiation by the object and the production of secondary radiations.

To investigate the impact of the mass of skin being irradiated on the absorbed dose rate, two skin surface areas were considered: 1.1 mm^2, an area often used in experiments, and 1 cm^2, an area recommended for use in radiation protection by ICRP.

The absorbed dose rate is dependent on the energy deposited in the skin. The model simulations for 1.5 MeV photons (Figure 5) showed that the energy absorbed in the 1 cm^2 tallies is about a factor of 6 greater than the energy deposited in the 1.1 mm^2 tallies at 70 µm

depth with this increasing to a factor of 10 below 300 μm. For low energy (0.01 MeV) photons, the ratio is only a factor of 2 at 70 μm depth increasing to a factor of 3 deeper in the skin. For 1.5 MeV electrons (Figure 8), the ratio between the energy deposited in the different area tallies is about a factor of 2 at 70 μm depth increasing to a factor of 4 at 400 μm. Low energy electrons (0.01 MeV) deposit roughly the same energy in both area tallies until deeper in the skin where a factor of 2 difference is present.

However, as the absorbed dose rate is energy deposited divided by the mass of tissue in the tally, which in the 1 cm^2 tally is about a factor of 90 larger than the mass in the 1.1 mm^2 tally, therefore the absorbed dose rate in the 1.1 mm^2 tallies is greater than that in the 1 cm^2 tally. For 0.662 MeV photons, this is a factor of about 30 at 50 μm depth and 15 at 375 μm. For 1 MeV electrons, this is a factor of 60 at 50 μm depth and 30 at 375 μm. This strong dependence on tissue mass averaging must be considered when evaluating the risk of severe tissue reactions occurring using a different target volume than the standard 1 cm^2 area calculation. However, care must be taken to avoid selecting a value for the tally area smaller than the area of the source object, because this can result in radiation from the sides of the object missing the tally area, as noted in section 4.2.

The model simulations with monoenergetic photons showed that the highest dose rates arise from low energy (0.01 MeV) sources, although sources of about 0.7 MeV produce roughly the same dose rate at skin depths below 150 μm (Figure 3). These dose rates are, however, several orders of magnitude lower than those produced by monoenergetic electrons of the same energy. This result confirms that the radiation protection practice of not considering photons in the calculation of local dose rate for contaminated skin is reasonable unless a detailed estimate of the dose rate is required.

The dose rate profiles for monoenergetic electrons show two different patterns, at low initial energies (< 0.3 MeV), representing the range of the primary electrons at shallower depths and then secondary photons in skin deeper in the skin (Figure 27). However, since even the primary electrons at 0.07 MeV energy penetrate the skin deeper than 50 μm, so the primary electrons are always the determinant of the dose rate at this depth. However, if assessing the dose deeper (> 300 μm) in the skin from electrons with energies lower than 0.3 MeV, the absorbed dose rate should be expected to be much lower.

Of the three types of radiation considered in this report, the highest absorbed dose rates in skin are produced by alpha particles. However, alpha particles only deposit their energy at shallow skin depths and the maximum depth reached is highly dependent on the energy of the alpha particle. Alpha particles with energies of less than about 6.5 MeV were found to be unable to penetrate the skin to depths of more than 50 μm, which is the shallow end of the range that ICRP recommends for general radiation protection purposes. This result confirms the information presented in ICRP Publication 116 (ICRP, 2010).

The MCNP results also show that alpha particles require an initial energy of 4 MeV and 8 MeV to penetrate skin to depths greater than 20 μm and 70 μm respectively (Figure 10). The risk of developing a negative response in the skin from exposure to alpha particles is therefore highly dependent on both the energy of the alpha particles and the location of

radiosensitive cells within the skin. For example, an object contaminated with radionuclides emitting alpha particles would pose a much lower risk if that object was in contact with skin on the soles of the feet than if it was in contact with skin on most other areas of the body. In addition, the presence of an object, contaminated with alpha emitting radionuclides, on the skin of infants and children may pose a much greater risk when compared to the same object present on the skin of an adult due to the relative thickness of the epidermis between these age groups. The current practice of not including energy deposited by alpha particles when assessing the dose rate in skin may result in an underestimation of the associated risk of a tissue reaction. Radionuclides, for which the contribution to the dose from alpha particles may be important, include ^{241}Am and ^{226}Ra which are found on small contaminated objects in the environment at several locations across the UK.

The material an object is composed of can affect the dose rate in skin due to self-absorption of some of the radiation. This work showed that it is the density of the object that has the most effect on the flux of radiation entering the skin, decreasing that flux by up to a factor of around 4 with a doubling of density, rather than the elemental composition of the object. This matches the observations of gamma ray dose rates from the ground by Saito and Jacob (1995).

The location of the radionuclide within the object also affects the dose rate in the skin as any radiation emitted by radionuclides away from the surface in contact with the skin may be absorbed or scattered by the material of the object. It was also shown that alpha radiation can irradiate the skin by travelling through the air around the object rather than by passing through it. Consequently, a dose can be received from a small radioactive object even if the object itself is of sufficient density and thickness to stop the alpha radiation. This may not be important for the majority of radiation protection assessments but can be important in specific circumstances, for example with > 5.5 MeV alpha sources and where doses to infants need to be considered.

6 Acknowledgements

This work was undertaken by staff in the Radiation Assessment Department of UKHSA's Radiation, Chemical and Environmental Hazards Directorate with additional advice from Rick Tanner and Jonathan Eakins (UKHSA).

7 References

Byrnes I, Lind OC, Hansen EL, Janssens K and Salbu B (2020). Characterization of radioactive particles from the Dounreay nuclear reprocessing facility. *Sci Total Environ* **727**, 138488.

COMARE (2014). *Committee on Medical Aspects of Radiation in the Environment (COMARE). Fifteenth Report. Radium contamination in the area around Dalgety Bay.* Public Health England.

Cooper JR, Randle K and Sokhi RS (2003). Radioactive Releases in the Environment: Impact and Assessment.

Dean PN, Langham J and Holland LM (1970). Skin Response to a Point Source of Fissioned Uranium-235 Carbide. *Health Physics* **19**(1), 3-7.

Dennis F, Morgan G and Henderson F (2007). Dounreay hot particles: the story so far. *Journal of Radiological Protection* **27**(3A), A3.

Environment Agency, Food Standards Agency, Food Standards Scotland, Natural Resources Wales, Northern Ireland Environment Agency and Scottish Environment Protection Agency (2022). *Radioactivity in Food and the Environment, 2021.* RIFE-27.

Goorley T, James M, Booth T, Brown F, Bull J, Cox LJ, Durkee J, Elson J, Fensin M, Forster RA, Hendricks J, Hughes HG, Johns R, Kiedrowski B, Martz R, Mashnik S, McKinney G, Pelowitz D, Prael R, Sweezy J, Waters L, Wilcox T and Zukaitis T (2012). Initial MCNP6 Release Overview. *Nuclear Technology* **180**(3), 298-315.

Harrison JD, Oatway WB, Brown IK and Hopewell JW (2023). Health risks from radioactive particles on Cumbrian beaches near the Sellafield nuclear site. *Journal of Radiological Protection* **43**(3), 031504.

Hopewell JW (1990). The Skin: Its Structure and Response to Ionizing Radiation. *International Journal of Radiation Biology* **57**(4), 751-773.

ICRP (1991a). 1990 Recommendations of the International Commission on Radiological Protection. ICRP publication 60. *Annals of the ICRP* **21**(1-3), 1-193.

ICRP (1991b). The Biological Basis for Dose Limitation in the Skin. ICRP Publication 59. *Annals of the ICRP* **22**(2), 1-104.

ICRP (1992). Radiological Protection in Biomedical Research. ICRP Publication 62. *Annals of the ICRP* **22**(3), 1-43.

ICRP (2002). Basic Anatomical and Physiological Data for Use in Radiological Protection: Reference Values. ICRP Publication 89. *Annals of the ICRP* **32**(3-4), 1-277.

ICRP (2007). The 2007 Recommendations of the International Commission on Radiological Protection. ICRP Publication 103. *Annals of the ICRP* **37**(2-4), 9-34.

ICRP (2008). Nuclear Decay Data for Dosimetric Calculations. ICRP Publication 107. *Annals of the ICRP* **38**(3), 9-96.

ICRP (2009). Adult Reference Computational Phantoms. ICRP Publication 110. *Annals of the ICRP* **39**(2), 1-164.

ICRP (2010). Conversion Coefficients for Radiological Protection Quantities for External Radiation Exposures. ICRP Publication 116. *Annals of the ICRP* **40**(2–5), 1-257.

ICRP (2012). ICRP Statement on Tissue Reactions and Early and Late Effects of Radiation in Normal Tissues and Organs — Threshold Doses for Tissue Reactions in a Radiation Protection Context. ICRP Publication 118. *Annals of the ICRP* **41**(1-2), 1-322.

ICRP (2015). Stem Cell Biology with Respect to Carcinogenesis Aspects of Radiological Protection. ICRP Publication 131. *Annals of the ICRP* **44**(3-4), 7-357.

Jaschke W, Schmuth M, Trianni A and Bartal G (2017). Radiation-Induced Skin Injuries to Patients: What the Interventional Radiologist Needs to Know. *Cardiovasc Intervent Radiol* **40**(8), 1131-1140.

Kaurin DG, Baum JW and Schaefer CW (1997). *Effects of radioactive hot particles on pig skin.* United States, NUREG/CR-6531; BNL-NUREG-52499; ON: TI98000162; TRN: 97:019500.

Kaurin DGL, Baum JW, Carsten AL and Schaefer CW (2001). Scab incidence on Pig Skin Resulting from Hot Particle Exposures under Varying Conditions. *Health Physics* **81**(1), 47-56.

McConn RJ, Gesh CJ, Pagh PT, Rucker RA and Williams III RG (2011). *Compendium of Material Composition Data for Radiation Transport Modeling.* Pacific Northwest National Laboratory, Richland, Washington, PNNL-15870 Rev. 1.

NCRP (1999). *Biological effects and exposure limits for "Hot Particles".* Washington, DC (USA).

Oatway WB, Brown J, Etherington G, Anderson T, Fell TP, Eslava-Gomez A, Hodgson A, Pellow P and Youngman MJ (2011). *Supporting Information for the Assessment of the Health Risks from Radioactive Objects on Beaches in the Vicinity of the Sellafield Site.* Health Protection Agency, Chilton (UK), HPA-CRCE-018 (supplement).

Oatway WB, Cabianca T and Jones AL (2020a). *Assessing the risk to people's health from radioactive objects on beaches around the Sellafield site. Summary report.* Public Health England, Chilton (UK), PHE-CRCE-056.

Oatway WB, Cabianca T and Jones AL (2020b). *Assessing the risk to people's health from radioactive objects on beaches around the Sellafield site. Technical report.* Public Health England, Chilton (UK), PHE-CRCE-057.

Particles Retrieval Advisory Group (Dounreay) (2012). *2012 Report.* SEPA.

Saito K and Jacob P (1995). Gamma Ray Fields in the Air Due to Sources in the Ground. *Radiation Protection Dosimetry* **58**(1), 29-45.

8 Appendix A

8.1 Photon point sources

In this section are shown the absorbed dose rates in different volumes of skin from exposure to a photon point source. The initial photon energies are 0.01, 0.1, 0.662 and 1.5 MeV.

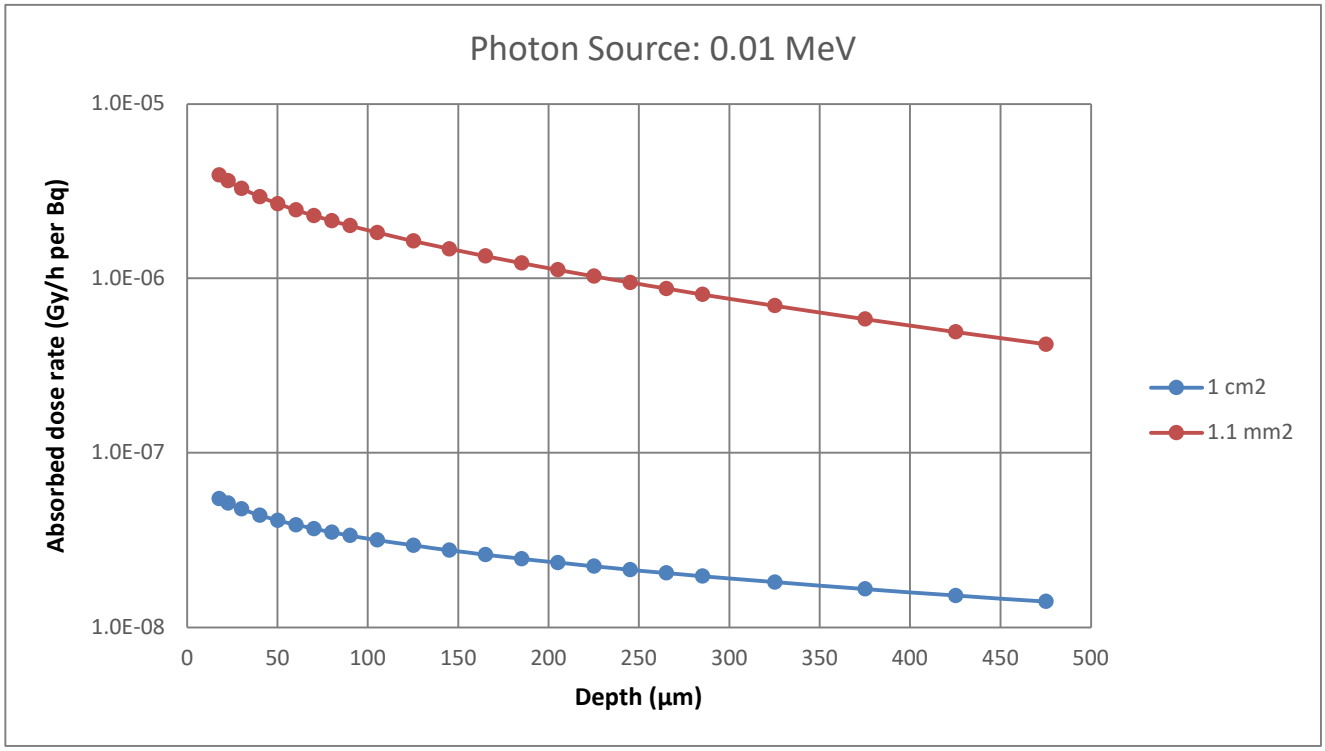

Figure 23: Absorbed dose rate by skin depth from 0.01 MeV photons for the different tally sizes

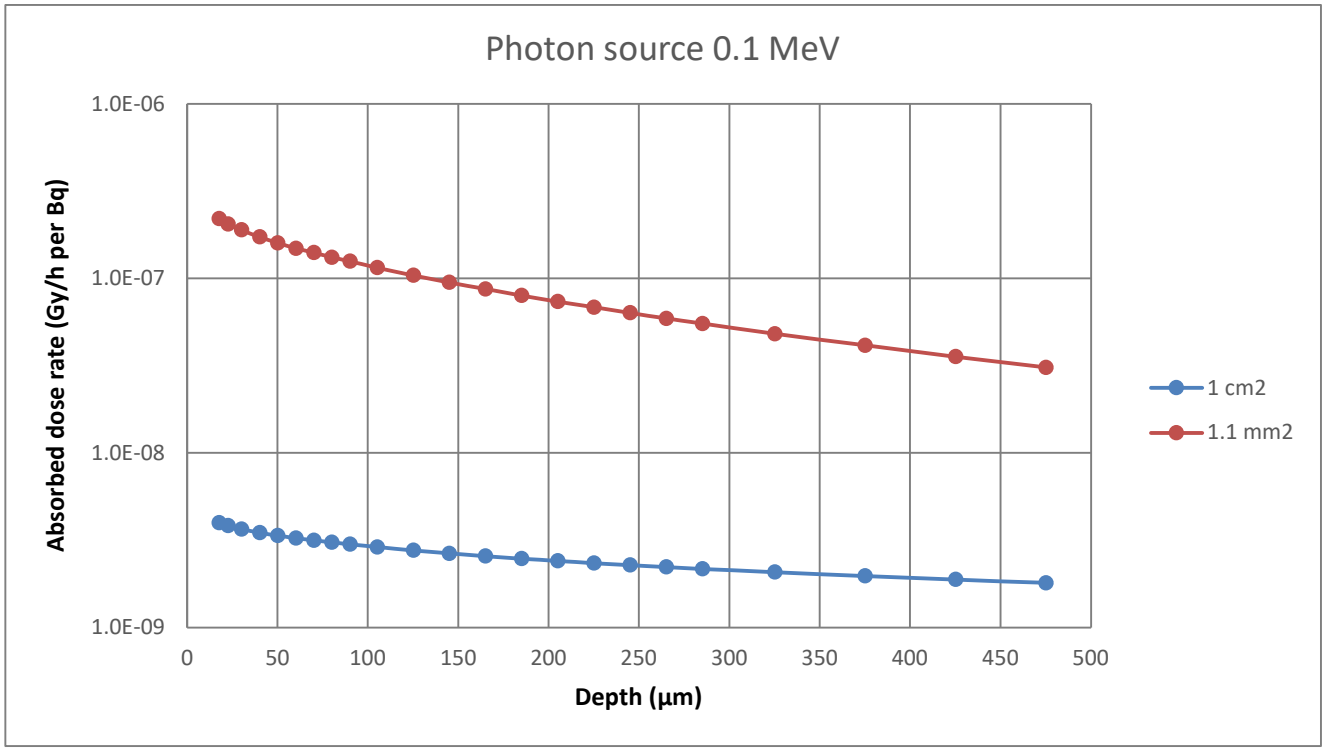

Figure 24: Absorbed dose rate by skin depth from 0.1 MeV photons for the different tally sizes

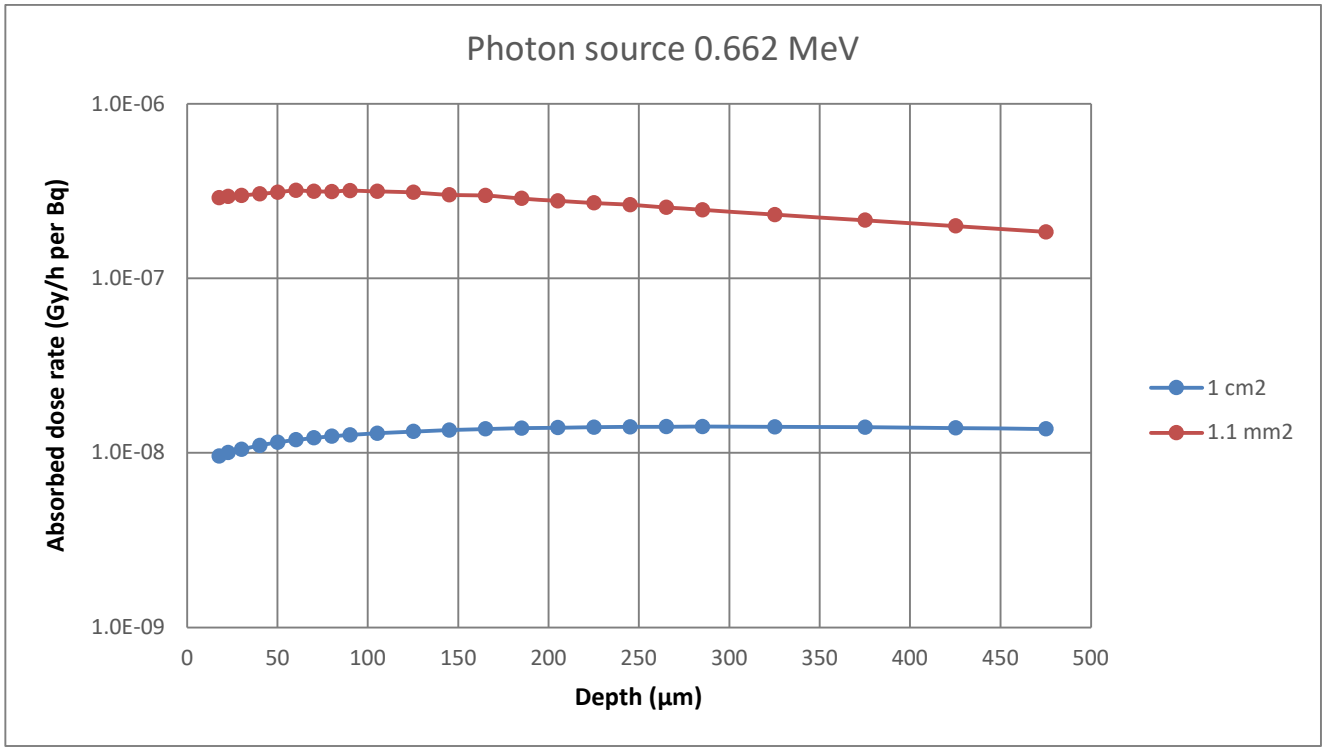

Figure 25: Absorbed dose rate by skin depth from 0.662 MeV photons for the different tally sizes

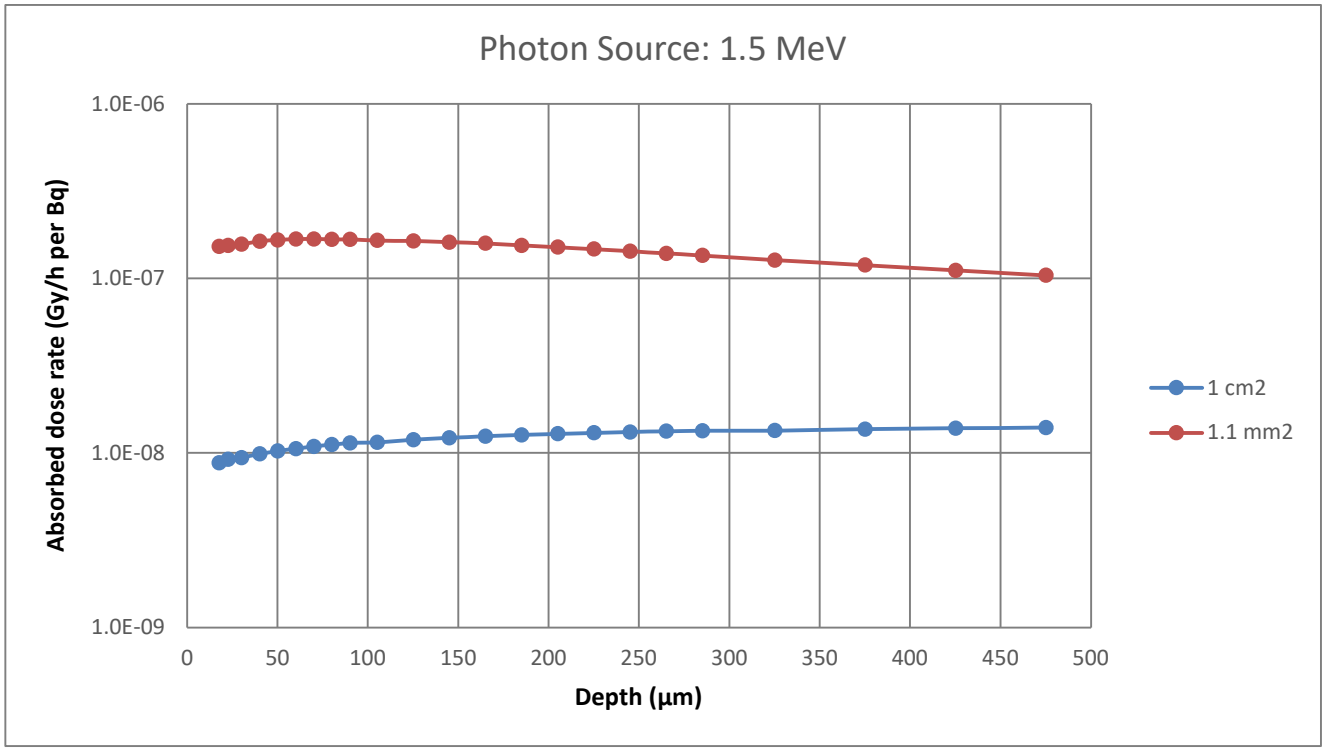

Figure 26: Absorbed dose rate by skin depth from 1.5 MeV photons for the different tally sizes

8.2 Electron point sources

Presented from Figure 27 to Figure 31 are the estimated absorbed dose rates in different volumes of skin exposed to a point source of beta radiation. The initial energies of the beta radiation are 0.07, 0.15, 0.3 and 1.0 MeV. The reduction in absorbed dose rate at the depths in skin seen for the 0.07 and 0.15 MeV point sources was found to be due to the range of the primary electrons.

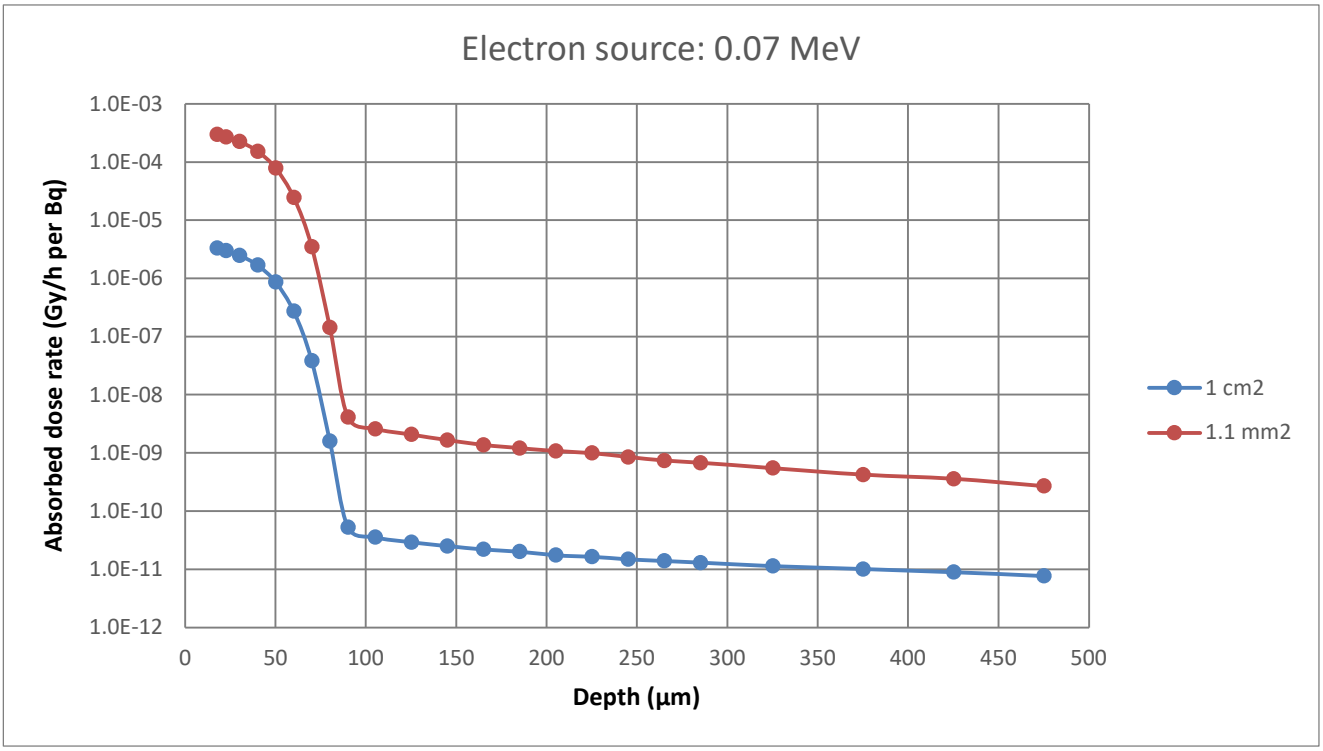

Figure 27: Absorbed dose rate by skin depth for a 0.07 MeV electron source for the different tally sizes

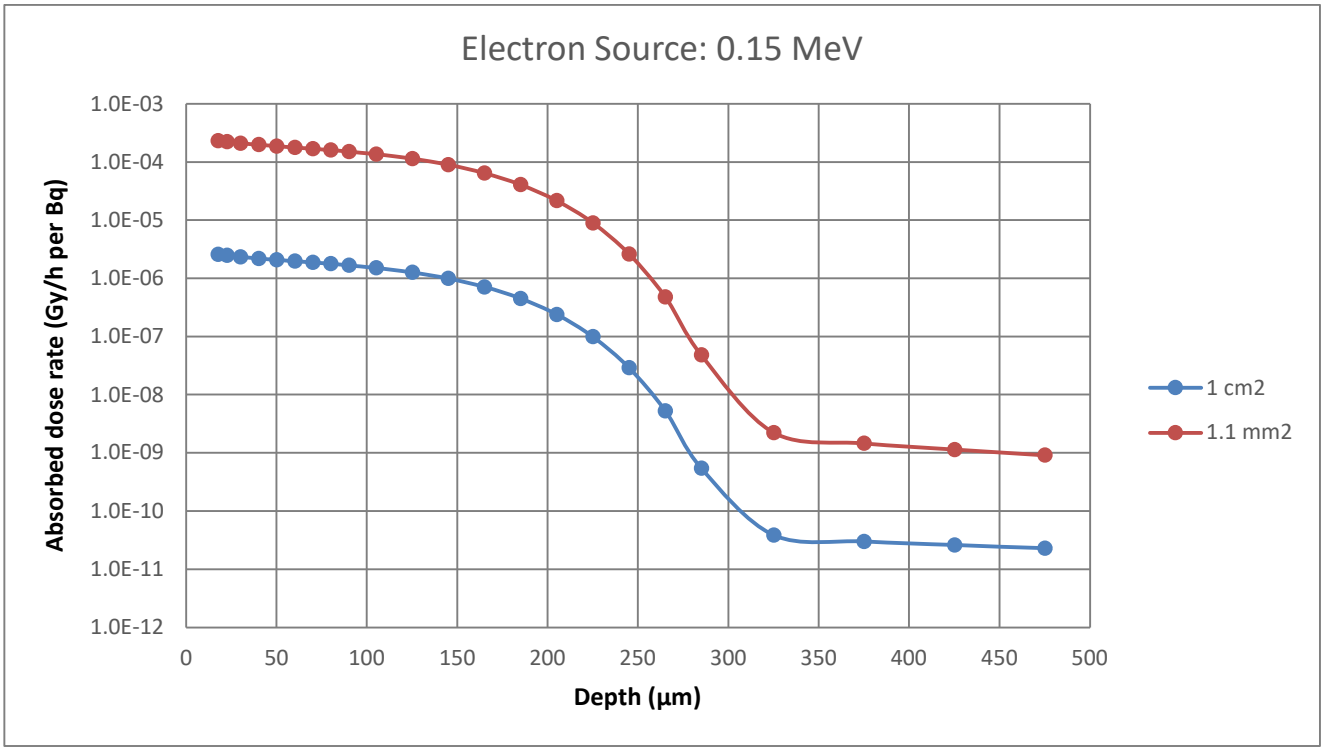

Figure 28: Absorbed dose rate by skin depth for a 0.15 MeV electron source for the different tally sizes

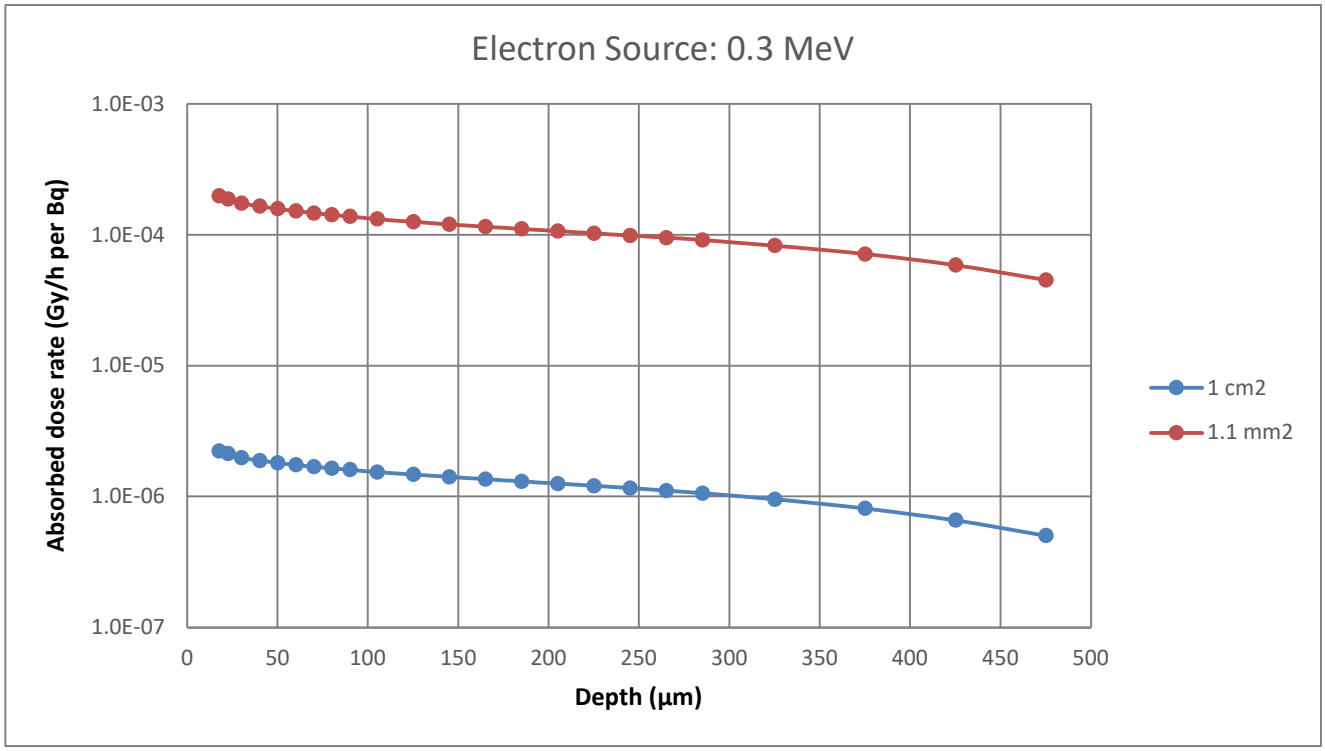

Figure 29: Absorbed dose rate by skin depth for a 0.3 MeV electron source for the different tally sizes

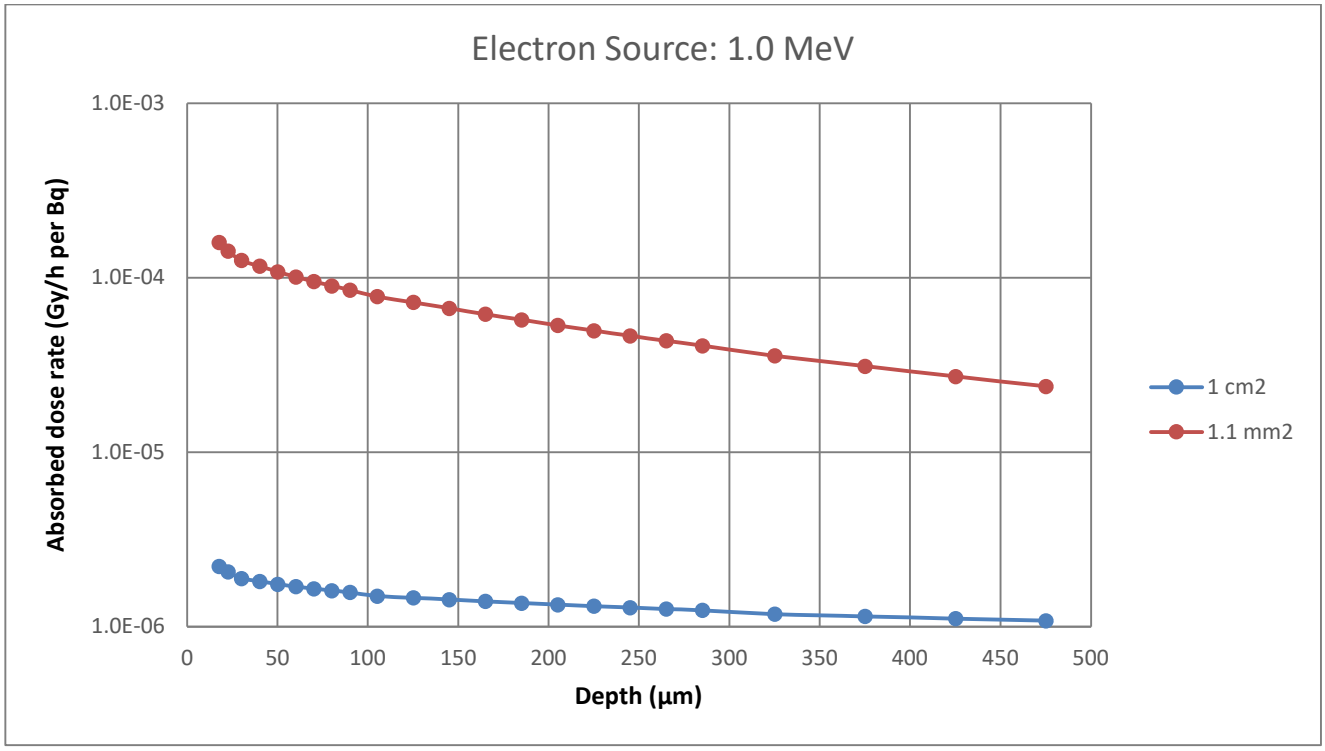

Figure 30: Absorbed dose rate by skin depth for a 1.0 MeV electron source for the different tally sizes

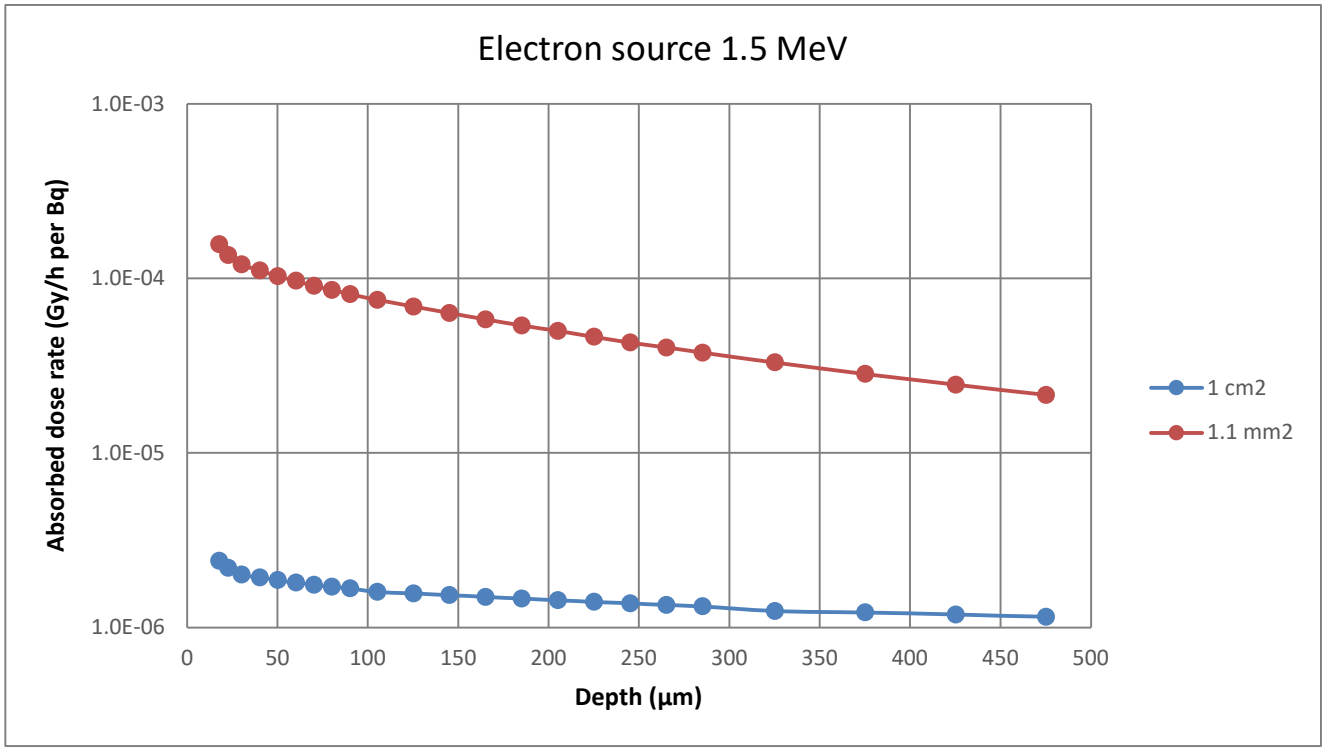

Figure 31: Absorbed dose rate by skin depth for a 1.5 MeV electron source for the different tally sizes

About the UK Health Security Agency

UKHSA is responsible for protecting every member of every community from the impact of infectious diseases, chemical, biological, radiological and nuclear incidents and other health threats. We provide intellectual, scientific and operational leadership at national and local level, as well as on the global stage, to make the nation health secure.

UKHSA is an executive agency, sponsored by the Department of Health and Social Care.

www.gov.uk/government/organisations/uk-health-security-agency

Version 1

Prepared by: Iain Brown
For queries relating to this document, please contact: Iain.Brown@ukhsa.gov.uk

Published: November 2024

Quality statement:
This work was undertaken under the Radiation Assessments Department's Quality Management System, which has been approved by Lloyd's Register Quality Assurance to the Quality Management Standard ISO 9001:2015, Approval No: ISO 9001 - 00002655.

UKHSA supports the Sustainable Development Goals